

**FUNCTIONAL PROPERTIES OF STRETCHABLE CONDUCTIVE INK (SCI) WITH
VARYING SUBSTRATE**



UNIVERSITI TEKNIKAL MALAYSIA MELAKA

**FUNCTIONAL PROPERTIES OF STRETCHABLE CONDUCTIVE INK (SCI)
WITH VARYING SUBSTRATE**

MUHAMAD ASYRAF BIN MOHAMED MUSTAFA




UNIVERSITI TEKNIKAL MALAYSIA MELAKA

2022

DECLARATION


I declare that this project report entitled "Functional Properties Of Stretchable Conductive Ink (SCI) With Varying Substrate" is the result of my own work except as cited in the references

Signature : 

Name : MUHAMAD ASYRAF BIN MOHAMED MUSTAFA

Date : 15/2/2022

UNIVERSITI TEKNIKAL MALAYSIA MELAKA



APPROVAL

I hereby declare that I have read this project report, and in my opinion, this report is sufficient in terms of scope and quality for the award of the degree of Bachelor of Mechanical Engineering

Signature : _____

Supervisor's Name : _____

Date : _____



UNIVERSITI TEKNIKAL MALAYSIA MELAKA

DEDICATION

To my beloved father and mother,

Mohamed Mustafa Bin Samad & Saripah Binti Mahamad Sarip



ABSTRACT

Stretchable conductive ink (SCI) is a functional material that enables the conductive ink film to have better electronic conductivity after stretching and folding. This project aims to investigate the effect of different polymer substrates on the functional properties of SCI. First, SCI's electrical and mechanical samples with varying GNP filler loading on Polyethylene (PET) and thermoplastic (TPU) substrates were prepared and tested. More specifically, the range of GNP filler loading used in this research is 5 wt.%, 7.5 wt.%, and 10 wt.%. Before the electrical and mechanical testing, the formulated SCI with different GNP filler loading was subjected to viscosity test by using a digital viscometer (MODEL 52DV). Besides, the hydrophobicity of the formulated SCI was investigated on the as-received PET and TPU substrate through a contact angle test using self-fabricated contact angle measuring. Then, the sample was characterised using a four-point probe to determine the SCI's sheet resistance (R_s), which refers to ASTM F390 as a guideline; meanwhile, mechanical properties were characterised through a quantitative 180° peel test using a universal testing machine. By formulating SCI using different GNP filler loading, the viscosity increases as the filler loading increases; however, low viscosity is not appropriate with the stencil printing method and affects the electrical properties of the printed SCI on the substrate. The electrical properties of SCI printed on TPU and PET substrate show a decrease in sheet resistance with increasing GNP filler loading, from 5 wt. % to 10 wt.%. However, the SCI printed on the TPU substrate exhibit better conductivity than the SCI printed on the PET substrate. There is a reduction in adhesion strength from the peel test with increasing GNP filler loading. In addition, the results suggest that the SCI exhibited higher adhesion strength when printed onto the PET substrates than on TPU substrates, possibly because of the hydrophilic nature of the polymer material. Such finding is directly correlated with the degree of wetting, based on the contact angle measured on PET, which is low and yield high adhesion strength. Overall, it can be concluded that the SCI printed on different substrates affect the functional properties of the SCI.

ABSTRAK

Dakwat konduktif boleh renggang ialah bahan berfungsi yang membolehkan filem dakwat konduktif mempunyai kekonduksian elektronik yang lebih baik selepas regangan dan lipatan. Projek ini bertujuan untuk mengkaji kesan substrat polimer yang berbeza pada sifat fungsi SCI. Pertama, sampel SCI dengan muatan pengisi GNP yang berbeza pada substrat Polietilena (PET) dan termoplastik (TPU) telah disediakan dan diuji dari segi sifat elektrik dan mekanikal. Secara lebih khusus, julat muatan pengisi GNP yang digunakan dalam penyelidikan ini ialah 5 wt.%, 7.5 wt.%, dan 10 wt.%. Sebelum ujian elektrik dan mekanikal, SCI yang dirumus dengan pengisi GNP yang berbeza telah dikenakan ujian kelikatan dengan menggunakan viskometer digital (MODEL 52DV). Selain itu, sifat kehidrofobikan SCI telah dikaji pada substrat PET dan TPU dengan kondisi sedia ada melalui ujian sudut sentuhan menggunakan pengukuran sudut sentuhan buatan sendiri. Kemudian, sampel dicirikan menggunakan kuar empat mata untuk menentukan rintangan helaian SCI (R_s), dengan merujuk kepada ASTM F390 sebagai garis panduan; sementara itu, sifat mekanikal dicirikan melalui ujian pengupasan 180° kuantitatif menggunakan mesin ujian universal. Dengan formulasi SCI menggunakan muatan pengisi GNP yang berbeza, kelikatan meningkat apabila muatan pengisi meningkat; walau bagaimanapun, kelikatan rendah tidak sesuai dengan kaedah cetakan stensil dan menjejaskan sifat elektrik SCI yang dicetak pada substrat. Sifat elektrik SCI yang dicetak pada substrat TPU dan PET menunjukkan penurunan rintangan helaian dengan peningkatan beban pengisi GNP, daripada 5 wt. % hingga 10 wt.%. Walau bagaimanapun, SCI yang dicetak pada substrat TPU mempamerkan kekonduksian yang lebih baik daripada SCI yang dicetak pada substrat PET. Terdapat pengurangan dalam kekuatan lekatan daripada ujian pengupasan dengan peningkatan beban pengisi GNP. Di samping itu, keputusan menunjukkan bahawa SCI mempamerkan kekuatan lekatan yang lebih tinggi apabila dicetak pada substrat PET berbanding substrat TPU, berkemungkinan disebabkan sifat hidrofilik bahan polimer. Penemuan sedemikian dikaitkan secara langsung dengan tahap pembasahan, berdasarkan sudut sentuhan yang diukur pada PET, yang rendah dan menghasilkan kekuatan lekatan yang tinggi. Secara keseluruhannya, dapat disimpulkan bahawa SCI yang dicetak pada substrat yang berbeza mempengaruhi sifat fungsian SCI.

ACKNOWLEDGEMENTS

Firstly, I would like to take this opportunity to express my sincere gratitude to my supervisor, Dr. Siti Hajar Binti Sheikh Md Fadzullah, whose contribution to stimulating suggestions and encouragement helped me to coordinate my project. I am grateful to her for her understanding, guidance, and insightful support in the development process.

I would also like to acknowledge with much appreciation my family and friends who invested their full support in me to complete this research.

A special thanks to Zuraimi, Andee, and Dani, postgraduate students who constantly share their knowledge and experience, primarily to experiment with this research. Appreciation is also given to all the technicians who contribute their expertise and dedicate their time to help me complete this research.



TABLE OF CONTENTS

DECLARATION	3
APPROVAL	4
DEDICATION	5
ABSTRACT	i
ABSTRAK	ii
ACKNOWLEDGEMENT	iii
TABLE OF CONTENTS	iv
LIST OF TABLES	vi
LIST OF FIGURES	vii
LIST OF ABBREVIATIONS	ix
LIST OF SYMBOL	x
CHAPTER 1	1
1.1 Background	1
1.2 Problem Statement	2
1.3 Objectives	4
1.4 Scope of Project	4
1.5 Planning and Execution	5
CHAPTER 2	7
2.1 Introduction	7
2.2 Stretchable Conductive ink	7
2.3 Conductive Filler	8
2.3.1 Metal-Based	9
2.3.2 Non-Metal Based	10
2.4 Polymer Binder	13
2.4.1 Epoxy	13
2.4.2 PEDOT: PSS	14
2.5 Substrate	15
2.5.1 Thermoplastic Polyurethane (TPU)	16
2.5.2 Polyethylene terephthalate (PET)	17
2.6 Properties of Stretchable Conductive Ink	18
2.6.1 Electrical Properties of SCI	18
2.6.2 Viscosity of SCI	19
2.6.3 Mechanical properties: Adhesion analysis	20
2.6.4 Wettability	22

CHAPTER 3	24
3.1 Overview of Research	24
3.2. Raw Materials	26
3.2.1 Conductive Filler	26
3.2.2 Conductive Polymer Binder	27
3.2.3 Solvents	28
3.2.4 Substrate Materials	29
3.3 SCI Preparation	30
3.3.1 Sample preparation for Electrical test.	34
3.3.2 Sample preparation for 180° Peel Test.	35
3.4 Viscosity Test	36
3.5 Contact Angle Test	37
3.6 Electrical Characterization	39
3.6.1 Four probe point test	39
3.7 Mechanical Characterization	40
3.7.1 180° Peel test	40
CHAPTER 4	42
4.1 Introduction	42
4.2 Viscosity of SCI with varying filler loading	42
4.3 Hydrophobicity study of different SCI's filler loading on PET and TPU substrate.	44
4.4 Electrical Performances of different SCI's filler loading on PET and TPU substrate.	48
4.5 Adhesion Performances of different SCI's filler loading on PET and TPU substrate.	51
CHAPTER 5	53
5.1 Conclusion	53
5.2 Recommendation	54
REFERENCES	55

LIST OF TABLES

TABLE	TITLE	PAGE
1.1	PSM I Gantt chart	4
1.2	PSM II Gantt chart	5
3.1	Specification of Graphene nanoplatelets conductive filler	25
3.2	Sigma Aldrich <i>PEDOT: PSS with 1.3 wt. % dispersion in H₂O</i>	26
3.3	Specification of TPU and PET substrate	28
3.4	Graphene- PEDOT: PSS SCI formulation for different filler and polymer loading	30
3.5	PEDOT: PSS Solution	30
4.1	Graphene filler loading and viscosity of SCI	42
4.2	SCI droplet behaviour on PET and the average contact angle	44
4.3	SCI droplet behaviour on TPU and the average contact angle	45
4.4	Graphene filler loading and average sheet resistance of SCI on PET and TPU substrate	48
4.5	Graphene filler loading and average maximum adhesion strength of SCI on PET and TPU substrate	50

LIST OF FIGURES

FIGURE	TITLE	PAGE
2.1	Classification of conductive filler with example	7
2.2	SEM images of 0D, 1D and 2D metal-based nanomaterial	8
2.3	Comparison of electrical property for various materials	9
2.4	Diagram of manufacture of GNPs starting from natural graphite	11
2.5	Chemical structure and schematic core-shell structure of PEDOT: PSS	14
2.6	Behaviour of TPU substrate after being applied mechanical	15
2.7	Molecular Structure of Polyethylene Terephthalate PET	16
2.8	Comparison of the recommended viscosity range for different printing	19
2.9	Peel test angle	20
2.10	Contact angle according to Young's equation	22
2.11	Wettability of liquid on the substrate	22
3.1	Flow chart of the methodology	24
3.2	Sigma Aldrich <i>PEDOT: PSS with 1.3 wt. % dispersion in H₂O</i>	26
3.3 (a)	Dimethyl Sulfoxide	27
3.3 (b)	Ethylene Glycol	27
3.3 (c)	Triton X-100	27
3.4	Mettler Toledo Analytical Balance	30
3.5	Planetary Centrifugal Mixer (THINKY MIXER ARE-310)	31
3.6	Flow process of SCI preparation	32
3.7	Dimension of prepared sample for electrical test	33
3.8	Dimension of prepared sample for 180° peel test	34

3.9	Illustration of sample for 180° peel test	34
3.10	Digital viscometer (MODEL 52DV)	35
3.11	Graphene-PEDOT: PSS SCI at set level of viscometer	35
3.12	Self-fabricated contact angle measuring tool	36
3.13 (a)	Sample of Contact Angle-TPU	36
3.13 (b)	Sample of Contact Angle-PET	36
3.14 (a)	ImageJ software	37
3.14 (b)	Contact angle measured at the right side of ink droplet	37
3.15	Four-point probe test	38
3.16	Illustration of probe head is placed on top of SCI surface	38
3.17	50 N Universal Tensile Machine (SHIMADZU AGS-X-HC)	39
3.19	Close-up view of 180°peel test sample set-up	40
4.1	Viscosity Vs filler loading of Graphene-PEDOT: PSS SCI	42
4.2	Average Contact Angle Vs Graphene-PEDOT: PSS SCI with different GNP filler loading and substrate	46
4.3	Average Sheet Resistance Vs Graphene-PEDOT: PSS SCI with different GNP filler loading and substrate	48
4.4	Average Maximum Bond Strength Vs Graphene-PEDOT: PSS SCI with different GNP filler loading and substrate	51

LIST OF ABBREVIATIONS

PCB	Printed Circuit Boards
SCI	Stretchable Conductive Ink
LED	Light Emitting Diode
TCF	Transparent conductive film
AgNWs	Silver Nanowires
CNT	Carbon Nanotube
GNP	Graphene Nanoplatelets
TPU	Thermoplastic polyurethane
PET	Polyethylene terephthalate
SEM	Scanning Electron Microscope
0D	Zero Dimension
1D	One Dimension
3D	Three Dimension
UV	Ultra Violet
PEDOT:PSS	Poly(3,4-ethylenedioxythiophene) Polystyrene Sulfonate
DMSO	Dimethyl Sulfoxide
EG	Ethylene Glycol

LIST OF SYMBOL

$^{\circ}\text{C}$	=	Degree Celsius
Ω	=	Ohm
sq.	=	Square
T_g	=	Glass temperature
m	=	Meter
μm	=	Micrometre
L	=	length
G	=	Correlation factor
I	=	Current
V	=	Voltage
R_s	=	Sheet Resistance
MPa	=	Mega Pascal
TPa	=	Tera Pascal
θ_{eq}	=	Contact Angle
γ_{SV}	=	Solid-gas surface tension
γ_{SL}	=	Solid-liquid surface tension
γ_{LV}	=	Liquid-gas surface tension



CHAPTER 1

INTRODUCTION

1.1 Background

Nowadays, technology is an essential part of our life. Technology has evolved in various ways, and it is certainly possible that it's getting better. People are always trying to improve everything that can benefit our lives. Without electronic devices, people's lives would be at stand still, and nothing would get done fast enough.

The development of electronic technology is growing rapidly, especially in printed circuit boards (PCBs). PCB is the main component of the electronic system that plays a vital role to support mechanically and electrically connected electronic components using conductive pathways, tracks, or signal traces etched from copper sheets laminated onto a non-conductive substrate (Hunrath & Forest, 2009). However, PCB is a conventional rigid electronic component limited to the wearable electronic industry to open up various applications, especially healthcare, energy, and military. It is because the rigid PCB cannot be stretched and bent. Therefore, with such a growing development in electronic technology, stretchable electronic devices are the new technology that can replace the use of PCB in the wearable electronic industry and directly leads to economic growth today and has positive effects on various aspects of daily life.

Generally, the stretchable electronic devices primarily consist of stretchable conductive ink (SCI), stretchable substrate, and an electronic circuit (i.e. resistor, LED, and capacitor) (Aziz et al., 2020). According to (Ding et al., 2020), SCI is a functional material that enables the conductive ink film to have better electronic conductivity after stretching and folding. This matter is caused by the effect of this ink that would aid in the automation and refinement of the manufacture of stretchable conductors and have a significant impact on flexible electronics. Other than that, the development of SCI has enabled a broad range of applications, for instance, the production of transparent conductive films (TCFs), flexible energy harvesting and storage, and wearable sensors. Moreover, it is due to SCI attractive features; it can be compressed, twisted, and adapted to complex non-planar surfaces besides the low manufacturing cost with high output (Huang & Zhu, 2019).

The SCI is classified into metal-based (i.e. silver, Copper and AgNws), carbon-based (CNT, Graphite and Carbon black) and hybrids of metal and carbon-based (i.e. Ag-PDMS and rGO-AGNP). (D. C. Kim et al., 2020) states that all of these types' mechanical and electrical performances depend on the size and shape of filler material. The best suitable filler material for the fabrication of SCI is nanomaterials and polymers with 1D long-chain structures (D. C. Kim et al., 2020). The 1D material can form junctions between the adjacent fillers and high conductivity. However, the stretchable substrate also plays a vital role in the fabrication of the SCI. From the literature, it was argued that an unsuitable substrate could affect the behaviour of the SCI (Aziz et al., 2020).

1.2 Problem Statement

The stretchable conductive inks (SCI) have received an increasing demand, especially in wearable sensors, due to their great flexibility and expendability while maintaining conductivity at high levels. In addition, stringent performances such as electrical

and mechanical required the fillers in SCI to be shifted from metallic to nanocarbon-based materials (Graphene and CNT) due to their remarkable characteristics (Wenting Dang et al., 2017). However, the replacement of metal fillers with nanocarbon-based materials is not fully explored in their functionality, performance, and durability on the various substrates.

Moreover, determining the viscosity of newly formulated SCI is essential because viscosity is the parameter determining the suitable printing method used to print the SCI onto the substrate (Khan et al., 2020). The unsuitable printing method used may affect the evenness of the SCI towards the substrate surface (Onggar et al., 2020). Conversely, there is limited solid data on the relationship between viscosity and printing methods that can affect SCI's electrical and mechanical properties printed on substrates. Thus, the viscosity of the SCI with different filler loading will be discovered by understanding the relationship between the SCI and the printing method.

Other than that, different substrates have different interface energy. The interface energy is related to the wetting and adhesion in which the wetting phenomenon influences the quality of printing and process reliability of the SCI (Yunos et al., 2020). The wetting phenomenon can be studied through the hydrophobicity of the SCI towards the substrate. However, there is still a lack of exploration on the hydrophobicity of the SCI on the polymer substrate, especially towards thermoplastic polyurethane (TPU) and Polyethylene terephthalate (PET).

Subsequently, numerous studies have been analysed and discussed regarding the SCI's performance that used polymer as a binder. Based on the previous study, the polymer binder reduces the conductivity of the SCI due to the high resistance of the polymer binder (Mohammed & Pecht, 2016). However, the replacement of polymer binder with conductive polymer binder like PEDOT: PSS is not fully explored in terms of electrical and mechanical

performance. Furthermore, filler content and the amount of polymer binder used in newly formulated SCI is vital to discover because they are the main factors that affect the functionality of the SCI (Merilampi et al., 2010).

Hence, this study aims to perform a comprehensive material characterization that serves as a baseline using newly formulated nanocarbon-based SCI for functionality and durability with varying substrate material.

1.3 Objectives

The objectives of this project are as follows:

1. To examine the viscosity of the SCI with different filler loading.
2. To study the hydrophobicity of the SCI with different filler loading towards varying substrates.
3. To evaluate the electrical and mechanical properties of the SCI with different filler loading on varying substrates

1.4 Scope of Project

The scopes of this project are:

- i. Formulation and fabrication of SCI on TPU and PET substrates.
- ii. The viscosity of SCI with different filler loading.
- iii. Contact angle test to determine the hydrophobicity of SCI on TPU and PET substrate.
- iv. SCI sheet resistance measurement by conducting a four-point probe test on printed SCI.
- v. SCI mechanical testing via 180° peel test.

1.5 Planning and Execution

Table 1.1 demonstrates the research planning and activities for PSM 1, including the process title selection, literature review for understanding the research related to the project, designing the experiment, report writing and submission, and finally, PSM I presentation. The research activities in PSM II started with the formulation of the samples, viscosity test, contact angle test, and then the material characterisation for electrical and mechanical properties for all samples. Lastly, all the data were analysed, and the results are discussed in this report. Research activities of PSM II are illustrated in Table1.2.

Table 1.1 PSM I Gantt chart

Week	1	2	3	4	5	6	7	8	9	10	11	12	13	14	15
Research Title Selection	■	■	■	■											
Literature Review		■	■	■	■	■	■	■	■	■	■	■	■	■	■
Methodology research study					■	■	■	■	■	■	■	■	■	■	■
Submission Progress Report							■								
Report Writing								■	■	■	■	■	■	■	
Report Submission														■	
PSM 1 Seminar															■

Table 1.2 PSM II Gantt chart

Week \ Activities	1	2	3	4	5	6	7	8	9	10	11	12	13	14	15
Literature Review	■	■	■	■	■	■	■	■	■	■	■	■	■	■	■
Formulation and Fabrication of SCI			■	■	■										
Characterization of the SCI <ul style="list-style-type: none"> • Viscosity test • Contact angle test • Sheet resistivity test • 180° peel test 					■	■	■	■	■	■	■	■	■		
Data Analysis							■	■	■	■	■	■	■	■	
Report Writing								■	■	■	■	■	■	■	
Report Submission														■	
PSM II Seminar															■

CHAPTER 2

LITERATURE REVIEW

2.1 Introduction

This chapter includes a review of several related research studies based on previous research. The main subtopics discussed in this chapter are the stretchable conductive ink (SCI), polymer binder, a conductive filler, and SCI's electrical and mechanical properties based on the previous study on this chapter.

2.2 Stretchable Conductive ink

According to Ding et al. (2020), SCI is a functional material that enables the conductive ink film to have better electronic conductivity after stretching and folding. This matter is caused by the effect of this ink that would aid in the automation and refinement of the manufacture of stretchable conductors and have a significant impact on flexible electronics. Next, the development of SCI has enabled a broad range of applications, for instance, the production of transparent conductive films (TCFs), flexible energy harvesting and storage, and wearable sensors. It is due to SCI attractive features; it can be compressed, twisted, and adapted to complex non-planar surfaces besides the low cost of manufacturing with high output (Huang & Zhu, 2019).

Subsequently, the most critical requirement of SCI is the ability to stretch after the sintering has taken place. It still maintains the electrical conductivity of the conductive filler. Furthermore, a good SCI is an ink that can strain at least 20% of its original length while maintaining electrical and mechanical performances (Mohammed & Pecht, 2016). It is a

good starting point for this nascent technology as 20% stretchability can meet many current requirements.

2.3 Conductive Filler

Conductive filler is the material used to fabricate conductive ink, which provides electrical conductivity to SCI. Therefore, the electric properties of SCI mainly depend on the type of conductive filler. However, the good conductive filler has superior inherent electrical properties: good charge transport capabilities, excellent electrical properties, inherent softness, and good mechanical properties.

There are two types of conductive used in SCI: metal-based and non-metal based. The non-metal based are divided into two, which are carbon-based and conducting polymer. Figure 2.1 shows the classification of conductive filler with examples.

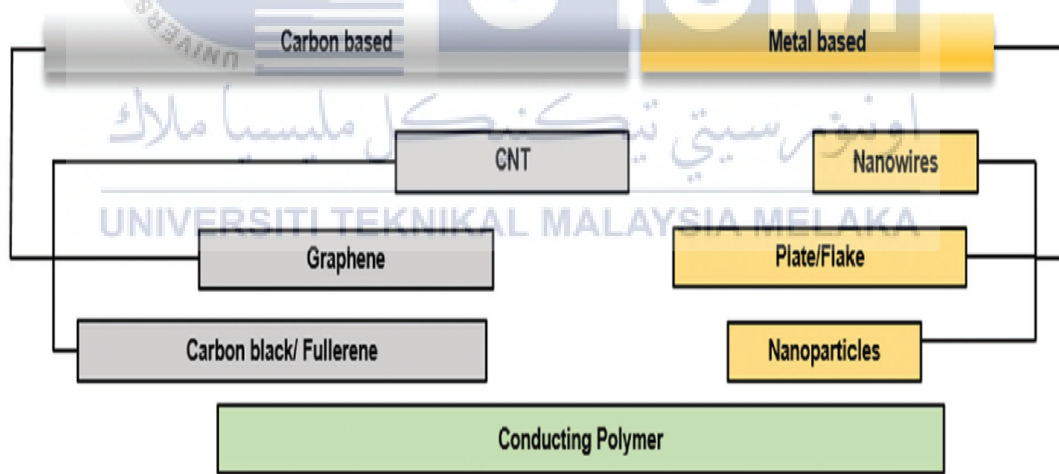


Figure 2.1: Classification of conductive filler with example (Choi et al., 2019)

2.3.1 Metal-Based

Metal-based nanomaterial is widely used as a conductive filler for SCI. It is because it has highly conductive and mechanical flexibility, such as Silver, Gold, and Copper. Conversely, it can be classified into three classes which are nanoparticles (0D), nanowires (1D), and nanoflakes (2D). Figure 2.2 shows the SEM images of 0D, 1D and 2D metal-based nanomaterials.

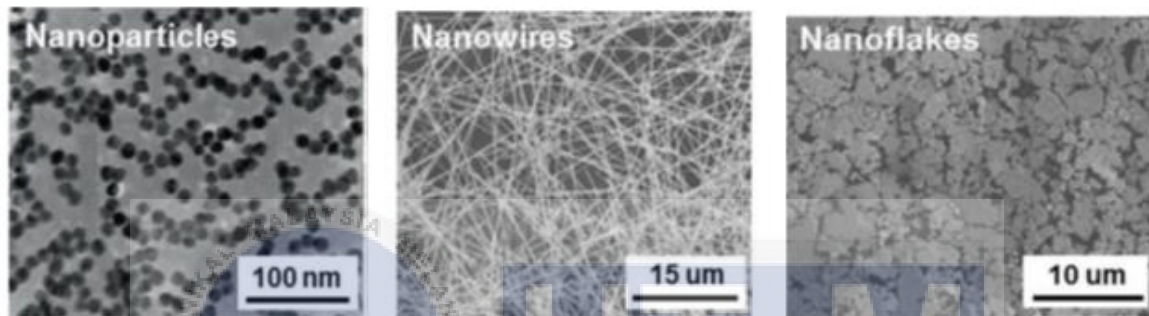


Figure 2.2: SEM images of 0D, 1D and 2D metal-based nanomaterial (D. C. Kim et al., 2020)

Among the three-dimensional metal-based nanomaterials, nanowires (1D) are commonly used as conductive fillers in SCI since they have the highest electrical conductivity compared to 0D and 2D metal-based materials. Examples of metal-based nanowires are silver nanowires (AgNWs), copper nanowires (CuNWs) and gold nanowires (AuNWs). According to (Choi et al., 2019), all the functional nanomaterial and polymers with 1D long chain structures can form a junction between the adjacent filler. Besides, it can provide a high level of conductivity with a small volume of fillers. Therefore, it shows that the 1D shape of the material can prevent the issue of increased loading of fillers in SCI.

The AgNWs and CuNWs are dynamically used to develop stretchable conductive composites such as flexible transparent conductive films, optoelectronic devices and molecular electronics. Due to their high intrinsic electrical conductivities, facile synthesis

on a large scale and low fabrication cost. Based on the previous study by (Hong et al., 2015), the AgNWs showed promising results on sheet resistance which is $15 \Omega/\text{sq}$. and transmission 95%. Nevertheless, there are a few disadvantages of using AgNWs as a conductive filler with high roughness, low adhesion to substrates, atmospheric corrosion, and degradation under UV and visible light (Azani et al., 2020).

2.3.2 Non-Metal Based

Non-metal based filler can be classified into carbon-based and polymer-based (i.e. polyaniline, PEDOT: PSS and polypyrrole). Both types can conduct electricity, but the carbon-based filler is widely used to fabric stretchable conductive composites because it has good electrical and mechanical properties compared to polymer-based. Carbon black, CNTs and Graphene-based filler are examples of carbon-based nanomaterial fillers with 0D, 1D and 2D shapes, respectively. Figure 2.3 shows that graphene and CNT have higher electric conductivity than most non-metal based fillers with low electrical conductivity. Therefore, even though other materials have low electrical conductivity, it is also frequently used for low electrical application.

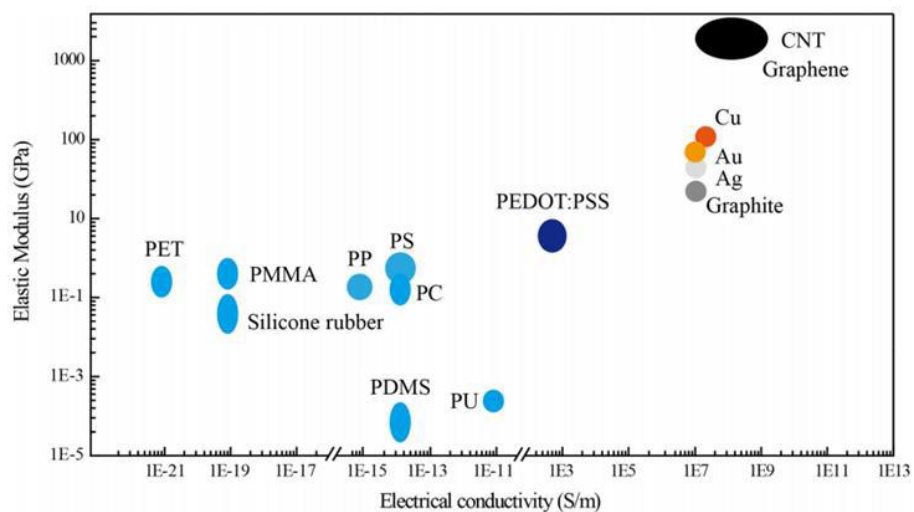


Figure 2.3 Comparison of electrical property for various materials (Wenting Dang et al., 2017)

2.3.2.1 Graphene

Graphene is a single freestanding monolayer of graphite. The 2D electron confinement inside a one-atom graphene layer gives it outstanding physical, electrical and mechanical properties. However, obtaining a good graphene dispersion in a polymer matrix is still a significant challenge. Based on the previous study by (Wang et al., 2019) where the study state that graphene has high thermal conductivity (5000 W/mK), high modulus of elasticity (1TPa), high electron mobility (25000 cm²/Vs) and electrical conductivity is more elevated than metal-based materials. However, the number of graphene layers and coupling effects from the underlying substrate influence the electronic characteristics of graphene (Cataldi et al., 2018).

Recently, graphene has been widely used in making electronic devices for various applications such as flexible, stretchable devices, low-cost printable electronics and high-frequency electronics. The reason is the atomic arrangement of the carbon atom in graphene allow its electron to easily travel at high velocity without a major chance of scattering (Cataldi et al., 2018).

Furthermore, graphene-based ink has been used to fabricate conductive components in printed electronics using inkjet printing, screen printing and gravure. Therefore, applying inkjet and gravure printing techniques on the graphene-based ink will produce an excellent graphene pattern. However, even though both of these techniques offer promising results, the screen printing technique is preferable as it requires low resistance. The reason is that the screen printing technique can produce a thick film (μm range) with a single pass and subsequently reduce producing time (Saad et al., 2020).

2.3.2.2 Graphene Nanoplatelets

Graphene nanoparticles (also known as graphite nanoplatelets, GNPs, or GPs) comprise a single and few-layer graphene combined with thicker graphite, as shown in Figure 2.4. Combining single and few-layer graphene and nanostructured graphite makes up the usual black powder formed during liquid-phase exfoliation and solvent evaporation. As a result, they are structurally hybrid between graphene and graphite.

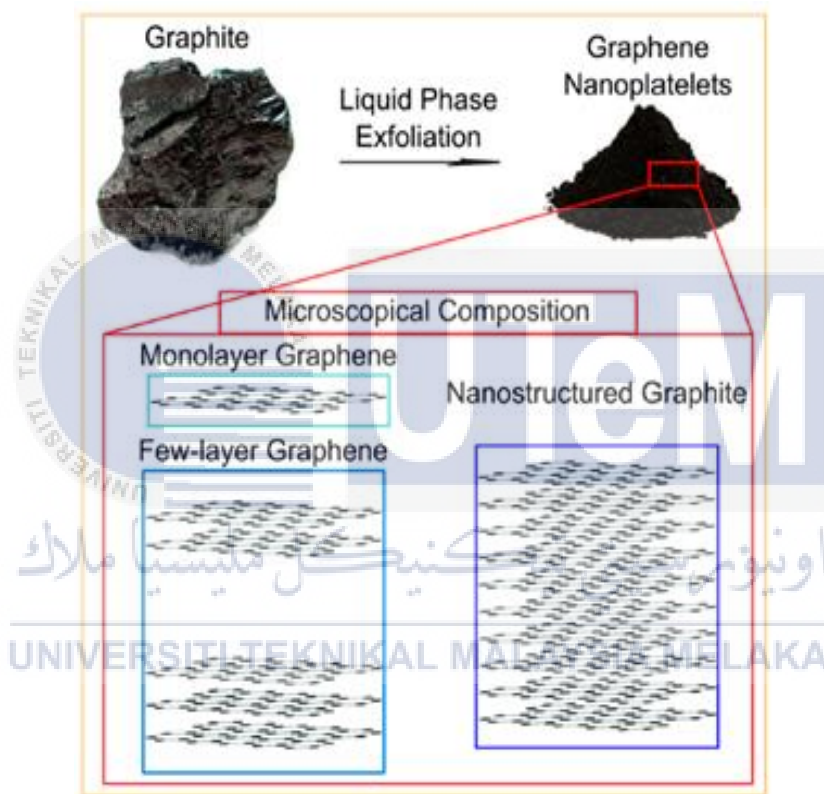


Figure 2.4 Diagram of manufacture of GNPs starting from natural graphite (Cataldi et al., 2018)

The GNPs are nanomaterials with attractive lightweight, high aspect ratio, and high electrical and mechanical properties. According to the previous study by Zhang et al., the study state that with the additional volume of 3.0% vol. of GNPs into PET, the electrical conductivity of 2.11 S/m was achieved. It shows that a small volume of GNPs can increase electrical conductivity.

Based on its properties, this type of material is very suitable to replace others nanostructure filler such as carbon black and carbon nanotubes in the fabrication of SCI. Besides that, the advantages of the GNPs are they can be easily and successfully incorporated into polymer matrices by solvents or melt compounding. It also showed good potential for enhancing the thermal conductivity of polymer matrixes and making them suitable as thermal interface materials.

2.4 Polymer Binder

Polymer binder is one of the essential materials used in SCI fabrication. Generally, the function of the polymer binder in SCI is to provide good adhesion strength between conductive ink and substrates and offer stretchability in the sintered state (Hsu et al., 2013). In addition, the adhesive connection must withstand the complete operating temperature range of the device and environmental factors that may be exposed during the use of the device (Hsu et al., 2013). Besides, a few properties are required for polymer binder: fast curing, high glass transition temperature elastic, and adequate moisture (Lim et al., 2017).

2.4.1 Epoxy

Epoxy is a type of thermosets polymer. Thermoset polymer is heavily cross-linked to produce a three-dimensional solid (3D) network structure (Kausar, 2017). There are a few advantages of using epoxy as an adhesive material: high resistance against high temperature, good adhesive strength, low cost, high mechanical properties, excellent bond strength, good adhesion to various substrates, and good chemical and moisture resistance. However, several disadvantages of epoxy are the thermal stability is limited to 185 to 200°C and can be brittle without modification (Huang & Zhu, 2019).

Besides, to produce a 3D structure stable polymer matrix using epoxy, heat radiation, ultraviolet (UV) light and curing agent is required during the curing process. The curing

agent is needed because it is a substance used to facilitate the bonding of the molecular components of the epoxy. Generally, there are several curing agents for epoxy: amines, anhydrides, dicyandiamide, melamine-formaldehyde, and catalytic curing agents, which are anhydride and amines the most common curing agents used (White, 1989). The curing agent for the epoxy depends on the curing condition, and specific physical properties are also required. However, the solvent is not required during the curing process as the solvent can produce air bubbles, leading to a significant decrease in the overall properties of the SCI (Hashemi & Mousavi, 2016).

2.4.2 PEDOT: PSS

PEDOT: PSS is an organic semiconductor prepared by doping cationic poly (3,4-ethylene dioxythiophene) and poly (4-styrene sulfonate) anion. According to (Hsu et al., 2013), the PEDOT: PSS is an intrinsically conductive polymer (ICP) that can be coated on various substrates and nanostructures. The PEDOT: PSS is widely used in the fabrication of SCI as a polymer binder. It is because of its high electrochemical, physical, and electrical properties. This statement can be proven by (Lim et al., 2017), where the study state that the PEDOT: PSS can be stretched to high elongations but suffer due to increased electrical resistance. However, PEDOT: PSS as a binder on metal nanopowder or metal nanowire will show much less electrical resistance despite limitations in the high elongation (Hu et al., 2020).

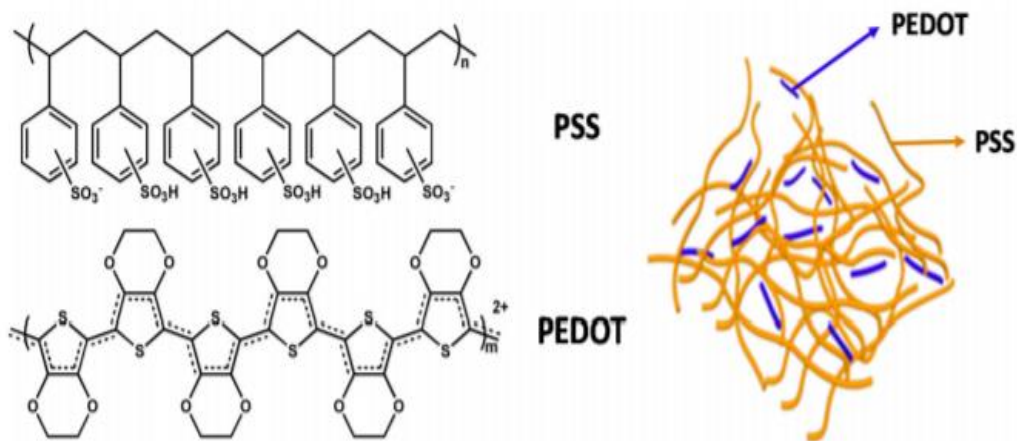


Figure 2.5: Chemical structure and schematic core-shell structure of PEDOT: PSS (Hu et al., 2020)

2.5 Substrate

The term substrate refers to the supporting material upon which the electronic components are attached or fabricated. In general, substrate use in electronic devices provides the interconnection to form an electronic circuit and cool the components' temperatures. Since the substrate plays a vital role in an electronic circuit, the material of the substrate should be able to withstand high currents and provide adequate voltage isolation. In other words, an unsuitable substrate can affect the behaviour of the interconnection components in the electronic circuit. It is because the behaviour of the interconnection components depends on insulating materials that can serve as a substrate.

Generally, the substrate types commonly used in printing the SCI are elastic substrates and plastic substrates. The elastic substrate is being used since the properties of these substrates that able to be permanently shaped, bent, or stretched uniaxially, biaxially, or radially after being applied mechanical force, as shown in Figure 2.6. In contrast, the plastic substrates cannot be permanently deformed after being stretched or compressed. Other than that, the suitable elastic substrate for SCI is the substrate that can stretch more than 200% strain (Aziz et al., 2020). As a result, the behaviour of the SCI is induced from

elastic substrates. According to Qi et al. (2021), the chemical and physical properties of the substrate also have a significant impact on the SCI's strain, which subsequently influences the overall performances of the SCI. (Wagner & Bauer, 2012) states that the chemical composition of the substrate's surface can affect the SCI's adhesion, and the substrate's structure can standardise the strain concentration in the SCI. However, there are still some questions about SCI's mechanical and electrical properties with varying substrates such as TPU and PET.

2.5.1 Thermoplastic Polyurethane (TPU)

Thermoplastic Polyurethane (TPU) is a thermoplastic elastomer that is one of the most rapidly expanding members of the polyurethane family. According to (Ashikin et al., 2018), TPU is a high-performance polymer used in coatings, adhesives, reaction injection moulding, fibres, and composites, among other applications. Since it has a high-performance polymer, the TPU also has high elastic properties, high abrasion resistance, low-temperature performances, and high shear strength. Furthermore, based on previous research by Ashikin et al. (2018), TPU is capable of withstanding a strain rate of up to 1000%. Therefore, TPU is a highly flexible material that can produce various physical asset combinations, valuable for multiple purposes.

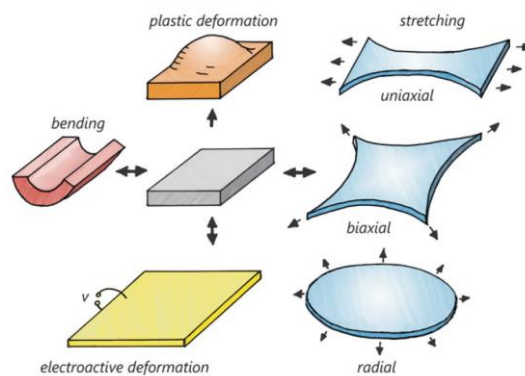


Figure 2.6 Behaviour of TPU substrate after being applied mechanical force (Wagner & Bauer, 2012)

2.5.2 Polyethylene terephthalate (PET)

Polyethylene terephthalate (PET) is a general-purpose thermoplastic polymer that belongs to the polyester family of polymers and is made through polycondensation of Purified Terephthalic Acid (PTA) with Ethylene Glycol (EG). The molecular structure of PET is $(C_{10}H_8O_4)_n$ as shown in Figure 2.7. The PET is used as a substrate material because of its exclusive features such as surfaces inertness, flexible film screen, good thermal stability, flexible film screen, high strength weight ratio and excellent moisture resistance. Furthermore, it has an excellent tensile strength of 55 to 75 MPa.

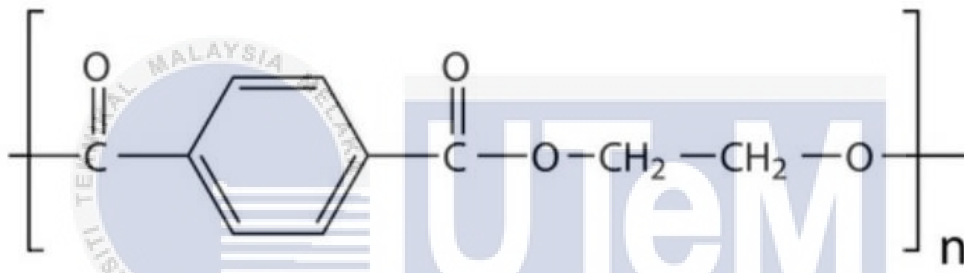


Figure 2.7: Molecular Structure of Polyethylene Terephthalate PET Chemical Formula:



The PET substrate is widely used in fabricating stretchable and flexible sensors such as antenna sensors by using printing technologies. The reason is that the PET substrate can decrease the production cost due to a reduction of the infrastructure needed, a decrease in the number of processing steps, and processing using the additive process at low temperature, which is 150-120°C.

2.6 Properties of Stretchable Conductive Ink

The properties of SCI can be characterised in terms of viscosity, wettability, electrical and mechanical properties.

2.6.1 Electrical Properties of SCI

In SCI, the most crucial property that needs to be concerned is electrical conductivity. The SCI is an interconnection material that fuses and is used to electronic bond connections. In general, electrical resistivity will be measured to determine the electrical conductivity of SCI. If the electrical resistivity decrease, the electrical conductivity of the SCI will be increased. The typical technique usually used to measure the electrical resistivity of SCI is the four-point probe test.

The SCI's resistivity depends on the volume fraction of conductive filler to induce the formation of the electrically conductive path in the SCI. As the volume fraction of conductive filler increases, SCI's resistivity decreases gradually. Besides that, different types of substrates used can affect the conductivity of the SCI. A previous study by A.s Ashikin et al. (2018) studied the effect of TPU and PET substrates on electrical properties of conductive ink and found that the factor of the curing process affects the thickness of the conductive ink on the substrates. Based on the previous study by Ismail et al. (2020), conductive ink on the stretchable and soft substrate has lower resistivity than the flexible substrate. As a result, the ink tends to shrink during the curing process and quickly pull the soft substrate to crumple closer. It also increases the contact surface between the particles and reduces the particle gap.

Moreover, filler content includes the particle size distribution shape, and orientation besides the amount of polymer binder used in conductive ink formulation will affect the conductivity of the conductive ink (Merilampi et al., 2010).

2.6.2 Viscosity of SCI

Viscosity is described as the degree of ink resistance to flow on the substrates or its ability to adhere to a surface of the substrates. According to Jason et al. (2015), the critical requirement in electronic ink is an optimum shear viscosity for smooth ink delivery to the substrate while maintaining trace conductivity. A highly viscous ink is sticky and does not flow easily because it strongly resists flow. On the other hand, the ink with not very viscous, has little resistance to flow and can flow easily and quickly on the surface of the substrates.

Based on the previous research by Khan et al. (2020), most of the electronic devices and sensors such as electronic circuits, light-emitting diode and solar cells are fabricated using ink with low viscosity (<100 cP). Low viscosity ink generally results in a smooth and pristine printed film. Besides, low-viscosity inks without binders enable the printing of high-purity materials. On the other hand, high-viscosity inks (1000–100 000 cP) are used mostly for fabricating conductive traces or passive electronic elements. In addition, high viscosity ink usually is formulated with binders and surfactants. The advantage of using high viscosity is that the conductivity of the ink can be improved by increasing the thickness of the ink in the hundreds of μm (Khan et al., 2020). In contrast, low viscosity inks have a limited thickness of $1\mu\text{m}$.

In addition, the viscosity of the ink and printing techniques are closely related to each other (Öhlund et al., 2014). Typically, low viscosity is printed using inkjet printing, blade coating, slot-die coating, and spray coating, while high viscosity can be printed using screen printing, stencil printing, or micro dispensing printing. Figure 2.8 compares the recommended viscosity range for different printing techniques.

Printing properties	Inkjet Printing	Screen Printing	Gravure Printing	Blade Coating	Spray Coating
Ink viscosity	5 – 50 cP	500 – 5000 cP	10 – 1000 cP	<100 cP	10 – 100 cP
Critical linewidth	30 – 70 μm	50 – 150 μm	5 – 100 μm	–	50 – 150 μm
Film thickness	0.1 – 1 μm	5 – 100 μm	0.1 – 1 μm	0.1 – 1 μm	0.5 – 1 μm
Film roughness	Low	High	Low	Low	Medium
Printing speed	0.01 – 0.1 m s^{-1}	0.1 – 1 m s^{-1}	0.1 – 10 m s^{-1}	0.01 – 1 m s^{-1}	0.1 – 1 m s^{-1}
2D patterning	Yes	Yes	Yes	No	Yes
Large-area scalability	Limited	Yes	Yes	Yes	Limited
Design flexibility	High	Low	Low	Medium	Medium

Figure 2.8: Comparison of the recommended viscosity range for different printing techniques (Khan et al., 2020).

2.6.3 Mechanical properties: Adhesion analysis

Adhesion performances between the SCI and the substrate can be analysed by qualitative or quantitative. The quantitative gives numerical data which can be interpreted without confusion. Meanwhile, qualitative gives numerical ranking based on visual assessment. Typically, the qualitative test used in the study is cross-cut, referring to ASTM D3359 as a guideline. The cross-cut test was evaluated by manually applying the tape to the test layer and quickly removed. The advantage of this test is no additional facilities are needed to run it. However, poorly controlled tape execution manually for this test leads to inaccurate results (Yurenka, 1962).

On the other hand, the qualitative test typically used in the study is the peel test. From this test, numerical adhesion strength can be analysed with the assistance of an appropriate universal tensile machine. The device was analysed by measuring the peel force load and securing the requesting peel angle. Common peel tests angles are shown in Figure 2.9. However, the pest test is usually used to evaluate the adhesion strength between SCI and substrate is the 180° peel test. Based on previous research by Eitner & Rendler (2016), higher forces were involved when the peeling angle was less than 90°, and less force was required at angle 135°.

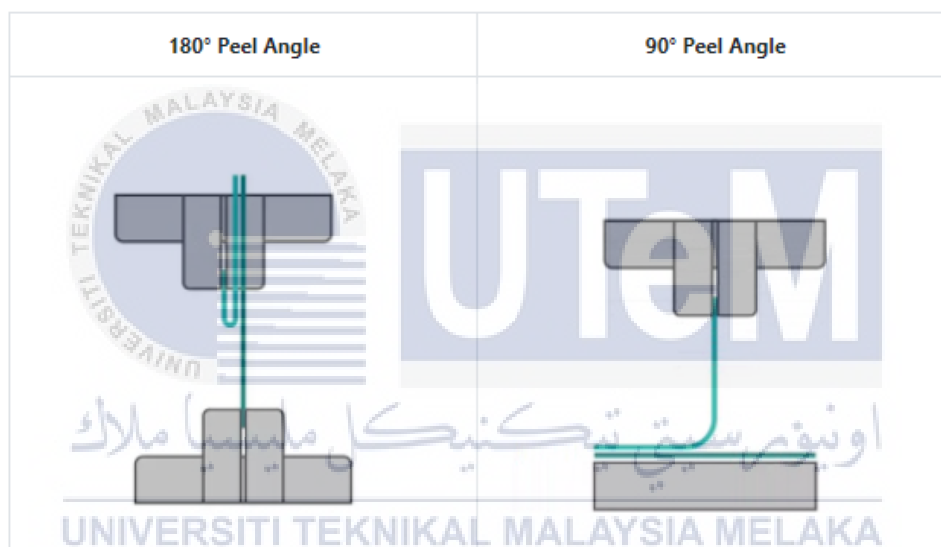


Figure 2.9: Peel test angle (Lauren, 2019)

2.6.4 Wettability

Wettability is the ability of a liquid to maintain contact with a solid surface. It is controlled by the balance between intermolecular interaction of adhesive type (liquid to the surface) and cohesive type (liquid to liquid). Wetting occurs only under two conditions: first, the liquid must not have a high viscosity, and second, the system's free energy must decrease after the wetting process. The wettability is determined by the degree of wetting or contact angle when a solid and liquid interacts.

The ink-substrate interface occurs when both the ink and the substrate come into contact by pressing the ink on the substrate. The optimal interface is highly dependent on the surface tension and surface energy of both the ink and the substrate (Yunos et al., 2020). The interface energy is related to wetting and adhesion. Young's equation describes the wetting phenomenon and the wetting phenomenon influencing the quality of printing and the conductive ink process reliability (Yunos et al., 2020).

The relationship between surface tension and the contact angle is defined as in Equation (2.1):

$$\theta = \cos^{-1}(n_1 n_s) \quad (2.1)$$

Young's equation was observed on the three-phase contact line as a mechanical force balance. As the liquid is dropped on a solid substrate, three different phases require three involvements for surface tension to be taken into consideration: (1) solid-liquid, (2) liquid-gas, and (3) solid-gas. Young's equation (Equation 2.2) describes the relationship between the contact angle (θ_{eq}) of the equilibrium with surface and three surface tensions as follows

$$\theta_{eq} = \frac{\gamma_{SV} - \gamma_{SL}}{\gamma_{LV}} \quad (2.2)$$

Where γ_{SV} , γ_{SL} , and γ_{LV} represent solid-gas surface tension, solid-liquid surface tension, and liquid-gas surface tension, respectively (Bonn et al., 2009). The contact angle (θ_{eq}) influences the level of wetting, whereby the higher the contact angle, the poorer the wetting and adhesion (Geils et al., 2019). Figure 2.10 illustrates a contact angle formation based on the Young equation.

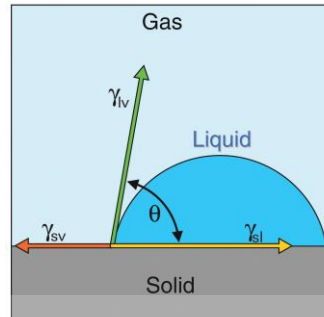


Figure 2.10: Contact angle according to Young's equation (Gould, 2003)

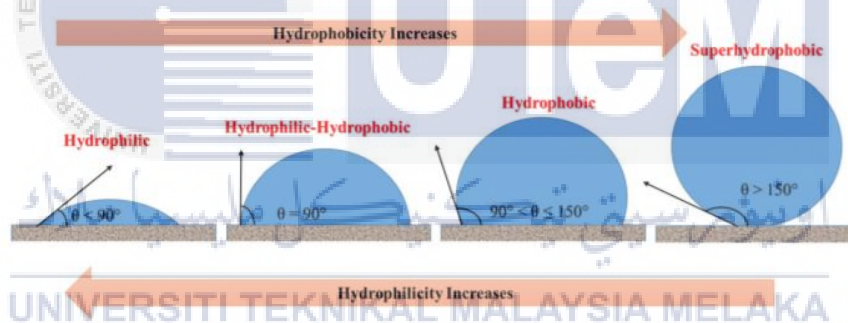


Figure 2.11: Wettability of liquid on the substrate (Doshi et al., 2018)

Figure 2.11 shows the conditions of wetting according to the contact angle. Hydrophobic, hydrophilic, superhydrophobic, and superhydrophilic are well-known wettability conditions that are always involved in the measurement of contact angles, indicating the degree of wetting. Contact angle less than 90° corresponds to high wettability, classified as hydrophobic or superhydrophobic. In contrast, a large contact angle or contact angle higher than 90° corresponds to low wettability categorized hydrophilic or superhydrophilic.

CHAPTER 3

METHODOLOGY

3.1 Overview of Research

This chapter discussed the details of the methodology for the experimental works involved in this research. The detailed methodology for this research project includes the type of Graphene, PEDOT: PSS and solvents used, and the SCI fabrication techniques described. In addition, the machine and apparatus used and the material characterisation tests conducted on the SCI with varying substrates are described too. Below is a summary of the research activities in this project are listed as follow:

The list of activities relating to the stage of Design the experiment (DOE) related to the research study are as follows:-

- I. Draft of experimental procedures for the research work, including identifying the variables and parameters of the experiments based on literature.
- II. Compilation of reference standards for relevant SCI characterisation.
- III. Compilation of material properties for graphene nanoparticle (GNP), which is used as a filler for the PEDOT: PSS matrix/ binder in the SCI formulation
- IV. Formulation and fabrication of SCI based on literature and past research
- V. Viscosity test to determine the viscosity of hybrid SCI with different filler loading.
- VI. Contact angle test to determine the hydrophobicity of SCI on TPU and PET substrate.
- VII. Preparation of the SCI samples for electrical and mechanical testing.
- VIII. Conduct electrical (four-point probe) and mechanical test (peel test) on all samples to compare the effect of filler loading in SCI on TPU and PET substrates.

IX. Collect and analyse the data

Figure 3.1 summarises the general methodology for this research, beginning with a literature review based on the study's title and ending with a report writing.

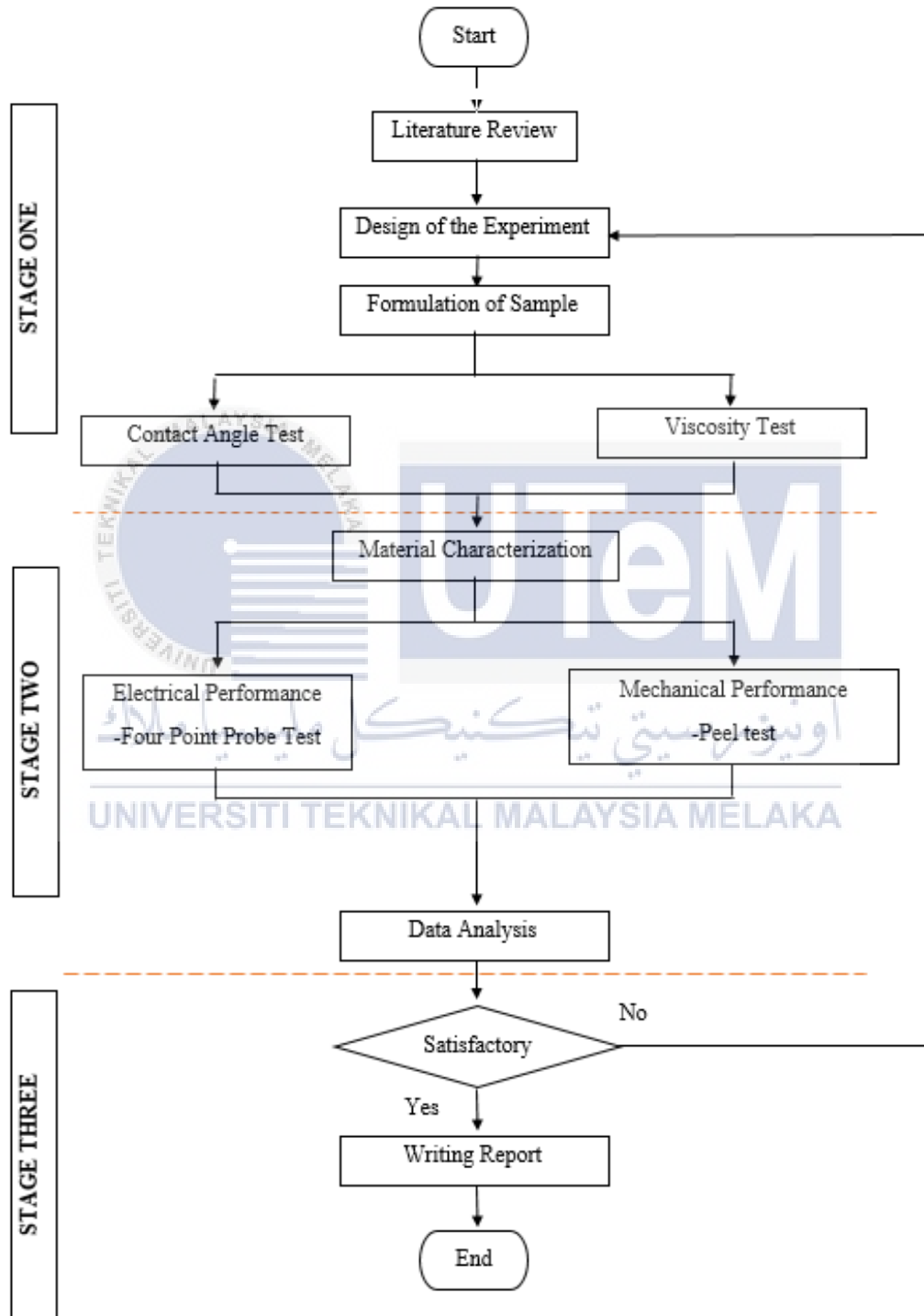


Figure 3.1: Flow chart of the methodology

3.2. Raw Materials

This research project uses three materials to fabricate hybrid SCI: conductive filler, conductive polymer binder, and solvents. Graphene Nanoplatelets with a size of 15 μ m was used as a conductive filler. Besides, the PEDOT: PSS was used as a polymer binder. Dimethyl Sulfoxide (DMSO), Ethylene Glycol (EG) and Triton x-100 were used as solvents. The last material is a substrate used to print the SCI on it. There are two substrates were used to run this research which is TPU and PET substrate

3.2.1 Conductive Filler

The type of conductive filler was used in the formulation of SCI is Graphene nanoplatelets with the size of the particle is 15 μ m. Sigma Aldrich supplies this conductive filler. This conductive filler can be easily incorporated into polymer binder by solvent or melt compounding and have good electrical and mechanical performances for SCI. Table 3.1 shows the specification of Graphene nanoplatelets conductive filler.

Table 3.1: Specification of Graphene nanoplatelets conductive filler

Criteria	Specification
Product Number	900420
Formula weight	12.01 g/mol
Colour	Dark Grey to Black
Form	Powder
Surface area	120-150 m ² /g
Acid Content	$\leq 0.5\%$

3.2.2 Conductive Polymer Binder

The type of conductive polymer binder was used in this research is PEDOT: PSS with 1.3 wt. % dispersion in H₂O which Sigma Aldrich supplies. Table 3.2 shows the specification of PEDOT: PSS with 1.3 wt. % dispersion in H₂O.



Figure 3.2: Sigma Aldrich *PEDOT: PSS with 1.3 wt. % dispersion in H₂O*

Table 3.2: Specification of PEDOT: PSS with 1.3 wt. % dispersion in H₂O

Criteria	Specification
Product Number	768650
Colour	Dark to very dark blue and black
Form	Paste
Residual Evaporation	4-6%
Resistivity	≤130 ohm.sq
Viscosity	≥50000 mPa.s
Optical Density	≤20

3.2.3 Solvents

The solvents used were Dimethyl Sulfoxide (DMSO), Ethylene Glycol (EG) and Triton X-100. The function of DMSO is to enhance the conductivity of SCI. The EG and Triton X-100 were added to improve the viscosity and surface tension and prevent SCI from drying and clogging.

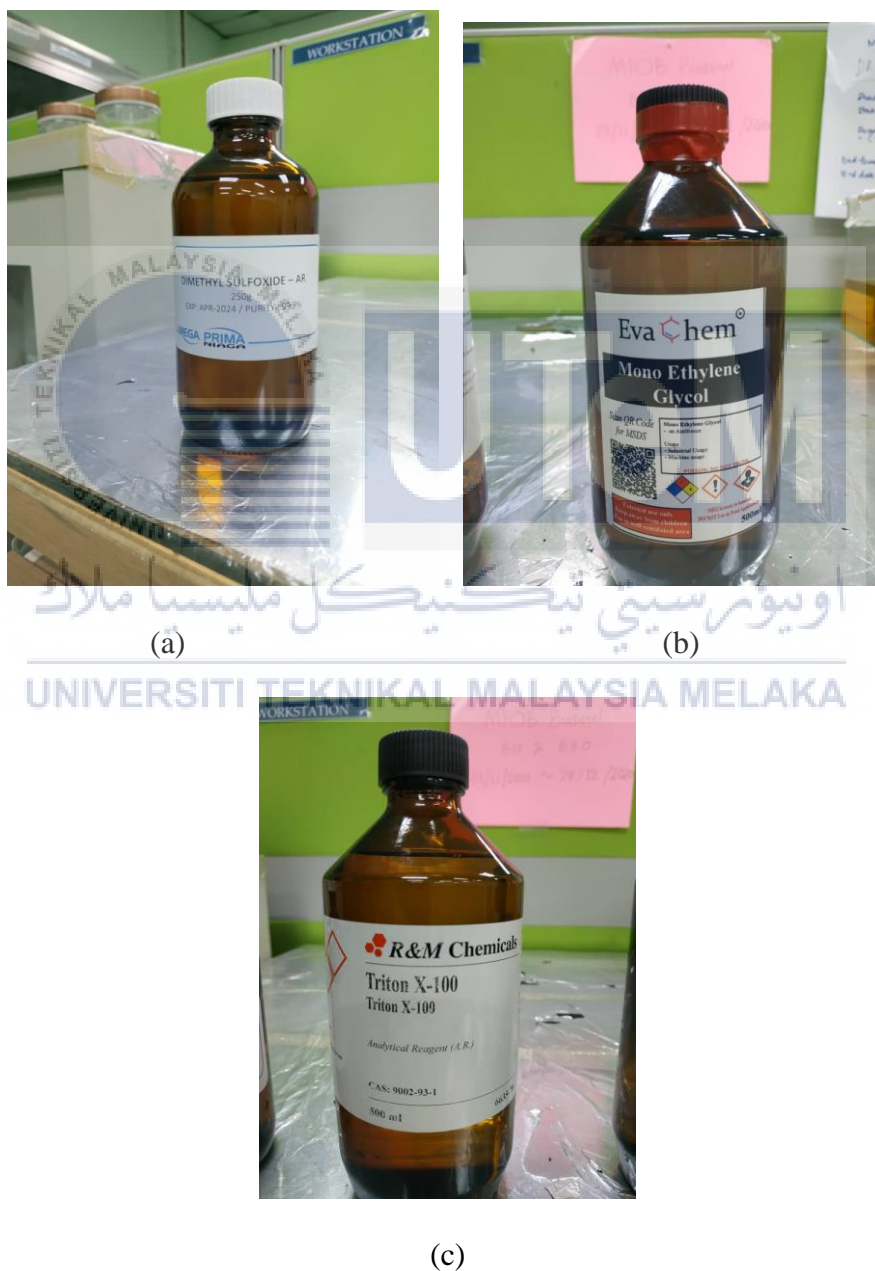


Figure 3.3: Solvents (a) Dimethyl Sulfoxide, (b) Ethylene Glycol and (c) Triton X-100

3.2.4 Substrate Materials

The substrate materials used in this research study were TPU and PET substrate. Although PET and TPU are from the same family, the critical difference is that TPU possesses both flexible and stretchable properties while PET provides a solid and rigid base. Thus, both materials were selected as the substrate for this research study. Table 4 shows the specification of TPU and PET substrate.

Table 3.3: Specification of TPU and PET substrate.

Criteria	TPU	PET
Materials	Thermoplastic polymer	
Physical Properties	Soft and stretchable polymer film	Hard, flexible, but not stretchable film
Supplier	Takedo Sangyo	Katco Lohmann
Grade	Tough Grace-TG88-1	Melinex 505
Thickness	100 μ m	100 μ m
Appearance	Transparent	Transparent
Resistivity	Dielectric	Dielectric

3.3 SCI Preparation

To formulate the Graphene-PEDOT: PSS ink, the Graphene Nanoplatelets, PEDOT: PSS, and solvents (DMSO, EG, and Triton-100) need to be combined correctly. Therefore, the first step to combine these materials is to calculate the amount of the materials in terms of weight percentage. The amount of the material was calculated using the Rule of Mixture as written in Equation (3.1):

$$X_c = X_m V_m + X_f V_f \quad (3.1)$$

Volume Fraction is expressed in Equation (3.2) and Equation (3.3)

$$\text{matrix volume fraction} = \frac{V_m}{V_c} \quad (3.2)$$

$$\text{Filler volume fraction} = \frac{V_f}{V_c} \quad (3.3)$$

Rule of SCI Mixture in Eq. (3.4) and Eq. (3.5):

$$\text{Mass of SCI} = \text{Mass of Graphene} + \text{Mass of PEDOT: PSS solution} \quad (3.4)$$

Mass of PEDOT: PSS solution

$$\begin{aligned} &= \text{Mass of PEDOT: PSS} + \text{Mass of DMSO} + \text{Mass of EG} \\ &+ \text{Mass of Triton X}_{100} \end{aligned} \quad (3.5)$$

All the samples were prepared first by mixing PEDOT; PSS with Dimethyl Sulfoxide (DMSO), ethylene glycol (EG) and triton x-100 by following the weight percentage shown in Table 3.4 (Seekaew et al., 2014). The amount of PEDOT: PSS, DMSO, EG, and triton x-100 needs to be measured using weight balance, as shown in Figure 3.4. The GNP filler loading chosen for this research is 5wt.%, 7.5wt.% and 10wt.%. Tables 3.4 and 3.5 below show each material's weight to formulate 5 g of SCI according to each filler.

Table 3.4: Graphene- PEDOT: PSS SCI formulation for different filler and polymer loading.

Sample	SCI mass, g	Graphene (wt.%)	Graphene mass, g	PEDOT:PSS solution (wt.%)	PEDOT: PSS Solution Mass, g	Substrates
1	4	5	0.2	95	3.8	PET and TPU
2	4	7.5	0.3	92.5	3.7	
3	4	10	0.4	90	3.6	

Table 3.5: PEDOT: PSS Solution (Seekaew et al., 2014)

PEDOT: PSS solution Mass, g	PEDOT: PSS (wt.%)	PEDOT: PSS Mass, g	DMSO (wt.%)	DMSO mass, g	EG (wt.%)	EG mass, g	Triton X-100 (wt.%)	Triton X-100 (wt.%)
3.8	89.82	3.413	5.98	0.2272	3.99	0.1516	0.199	0.00756
3.7	89.82	3.323	5.98	0.2213	3.99	0.1476	0.199	0.00736
3.6	89.82	3.234	5.98	0.2153	3.99	0.1436	0.199	0.00716



Figure 3.4: A Mettler Toledo Analytical Balance

After the solvents were added to the PEDOT: PSS, the mixture was transferred to the planetary centrifugal mixer (THINKY MIXER ARE-310) for 10 minutes at a speed of 400 RPM. Then, the amount of GNP needed was measured using weight balance and added to the PEDOT: PSS solution. The mixture was then blended and degassed using the planetary centrifugal mixer for another 10 minutes at a speed of 400 RPM. The Graphene-PEDOT: PSS SCI was ready for viscosity and contact angle tests.



Figure 3.5: A planetary centrifugal mixer (THINKY MIXER ARE-310)

After the viscosity test and contact angle were done, the formulated SCI with different filler loading was then printed to the TPU and PET substrate for the electrical and mechanical test. Then, the samples were placed inside the Memmert oven, which was readily heated with 60 °C to cure the hybrid SCI for 15 minutes. The curing process is needed to improve the bonding between the inks and polymer binder particles and improve the adhesion between the ink and the substrates. After being cured, the printed samples were left

aside to be fully dry at room temperature. After that, the samples are ready to be analysed.

The flow process of SCI preparation is illustrated in Figure 3.6

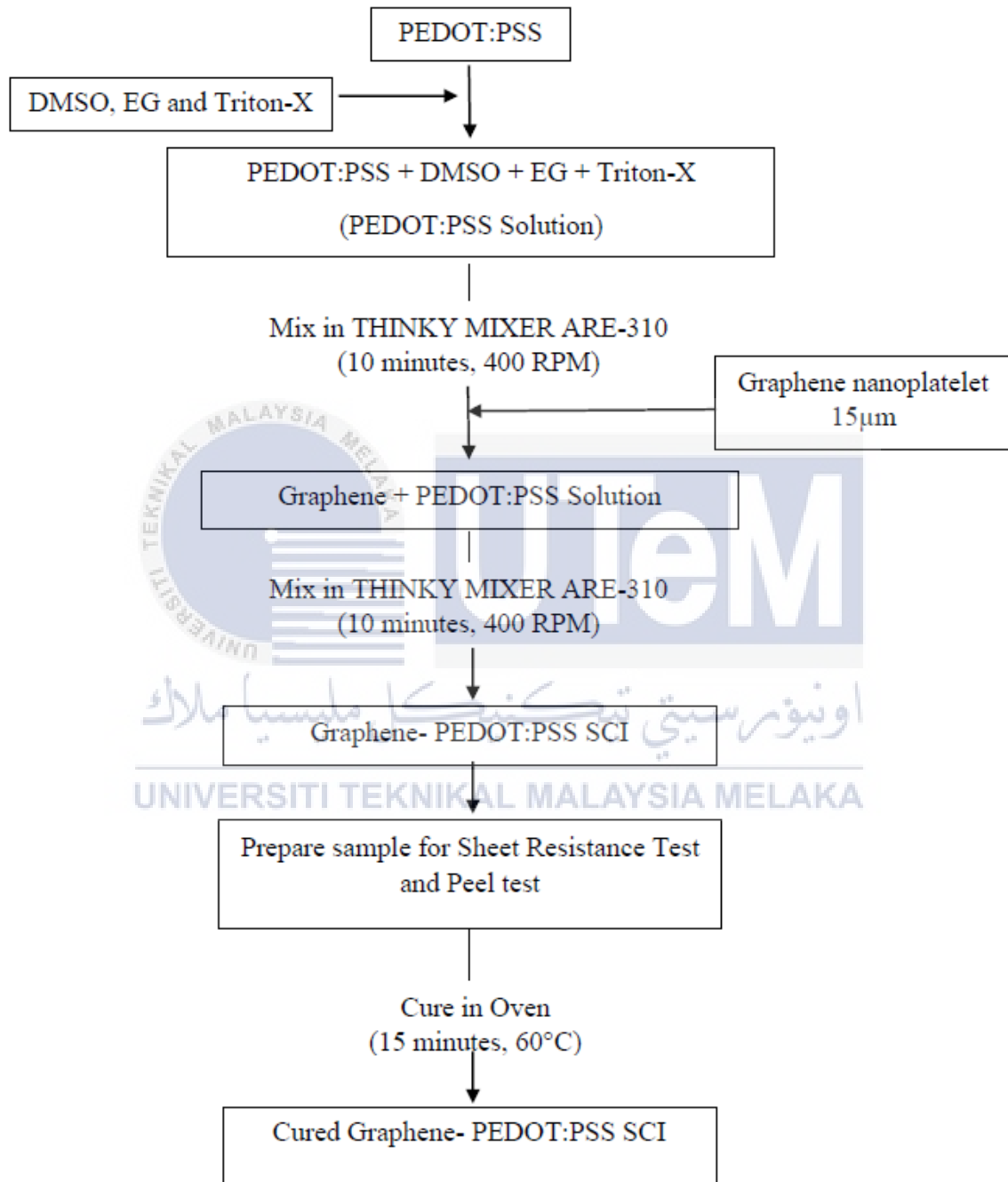


Figure 3.6: Flow process of SCI preparation

3.3.1 Sample preparation for Electrical test.

For the electrical test method, the testing standard of ASTM F390-11 was referred to as a guideline to measure the SCI's sheet resistance ($\Omega/\text{sq.}$) using a four-point probe test unit. The sample was prepared according to Figure 3.7. The Graphene-PEDOT: PSS ink sample was printed on the TPU and PET substrates with dimensions of 10 mm (width) and 40 mm (length) using the stencil printing technique.

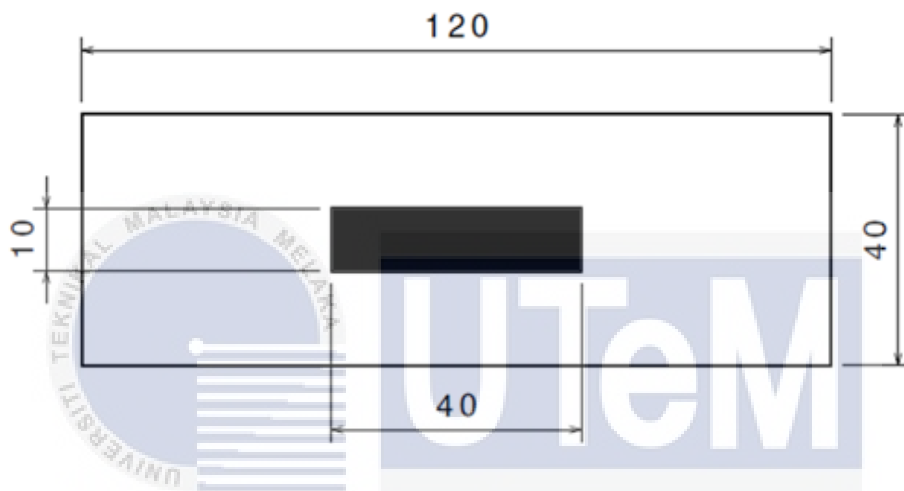


Figure 3.7: Dimension of prepared sample for electrical test

All the test samples contain 15 points along a 4.0 mm length of SCI. The thickness of the SCI was controlled using 2 layers of Scotch tape and spread using a razor blade for 2 consecutive times in one direction. To keep the thickness of Graphene-PEDOT: PSS ink at 0.1mm for all samples, the pressure, angle of the razor blade, and layer applied need to be constants. After that, the sample was cured using a Memmert oven at 60°C for 15 minutes.

3.3.2 Sample preparation for 180° Peel Test.

To fabricate the sample for the peel test, the Graphene-PEDOT: PSS ink sample was printed on the TPU and PET substrates with dimensions of 15 mm (length) and 20 mm (width) as illustrated in Figure 3.8 by using the stencil printing technique. The method for controlling ink thickness and curing process is the same as in Section 3.3.1.

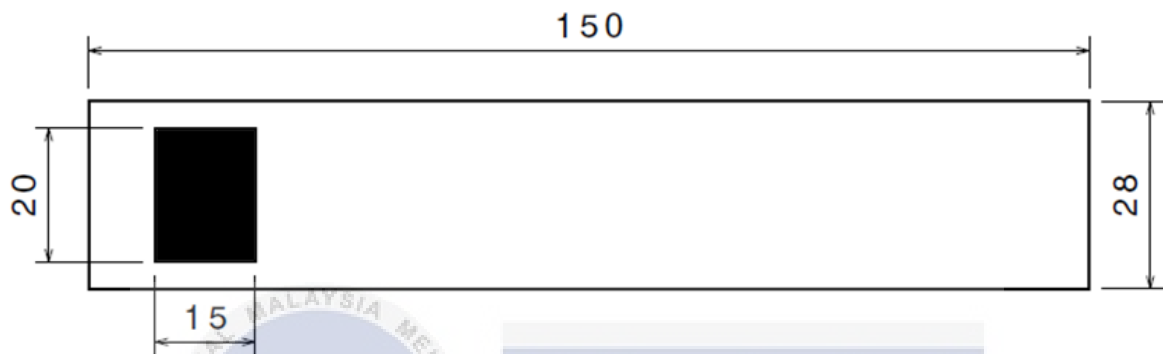


Figure 3.8: Dimension of prepared sample for 180° peel test

After the curing process, the printed Graphene-PEDOT: PSS ink was fixed on the glass slide with Epoxy 3M DP420 and was cured at room temperature for 2 hours. The Epoxy 3M DP420 was used because it has good adhesive strength for composites, long term durability and is easy to use.

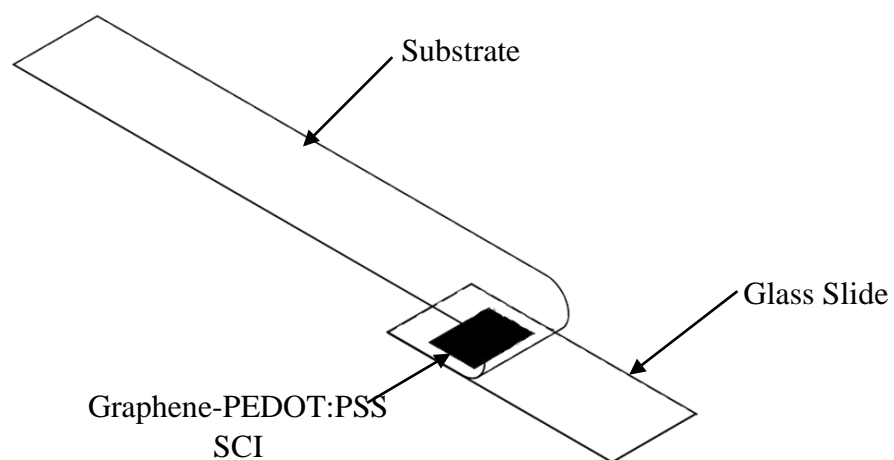


Figure 3.9: Illustration of sample for 180° peel test

3.4 Viscosity Test

Viscosity is a measure of fluid's resistance to flow. It is one of the essential properties of the SCI and plays a vital role in developing good SCI. In this research study, the viscosity of SCI with different filler loading was measured by a digital viscometer (MODEL 52DV), as presented in Figure 3.10.



Figure 3.10: Digital viscometer (MODEL 52DV)

After the ink formulation, the 4g of SCI was poured into a digital viscometer until the set level as presented in Figure 3.11. The measurement temperature was set at 40°C by the viscometer software. Then, the viscosity test was started by pressing the start button in viscometer software, and the ball began to rotate to measure the viscosity of SCI. The results for the viscosity test were shown in viscometer software.

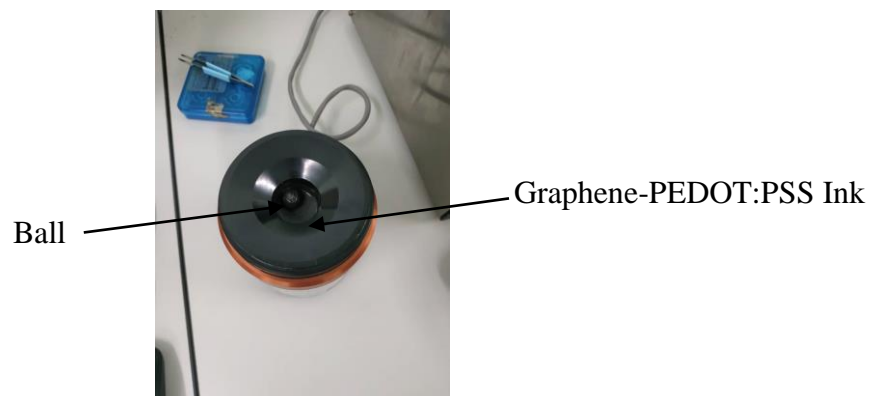


Figure 3.11: Graphene-PEDOT: PSS SCI at a set level

3.5 Contact Angle Test

The wettability study aims to measure the level of wetting when solid and liquid phases interact with each other. It measures the surface attributes of polymers and performs many essential tasks in printing and coating liquids. For this experiment, the contact angle test was run using a self-fabricated contact angle measuring tool as shown in Figure 3.12 to determine the wetting properties of the SCI with different filler loading on PET and TPU substrate. The substrates condition for this test is in receive condition without any heat treatment and surface treatment. Furthermore, ASTM D5725 was used as a guideline for this contact angle test.



Figure 3.12: Self-fabricated contact angle measuring tool

Before running the contact angle test, the PET and TPU substrate were cut into small pieces with the dimension of 28 mm width and 75 mm, as demonstrated in Figure 3.13.

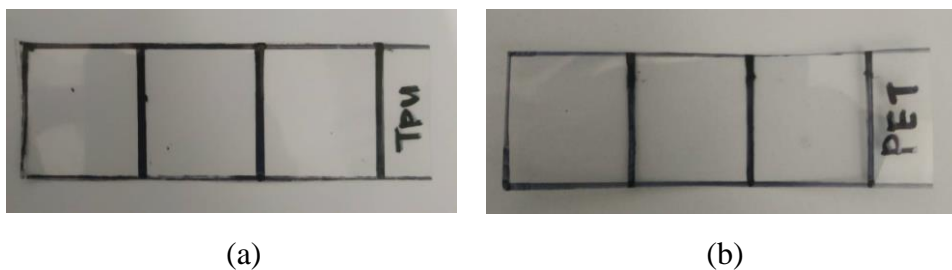


Figure 3.13: Sample of (a) TPU and (b) PET

After that, the upper surface for both polymer substrates was divided into 3 equal parts, 25 mm per part, using a permanent marker. This reason is to get the average data for the contact angle of SCI. Next, the distilled water and acetone were used to clean up the upper surface of both substrates and dried at room temperature.

Right after both substrates were dried, the contact angle test was run using self-fabricated contact angle measurement tools, as shown by dropping 0.5 μl on the upper surface of the substrate. The droplet image was snapped 3 times as the ink drop touched the substrate surface. The experiment was repeated for other surface parts for both substrates. The value of the contact angle is measured by ImageJ software by using three-point measurement, as presented in Figure 3.14 (a). The value of each ink contact angle was measured on the left side (S. Kim et al., 2011), as shown in Figure 3.14 (b).

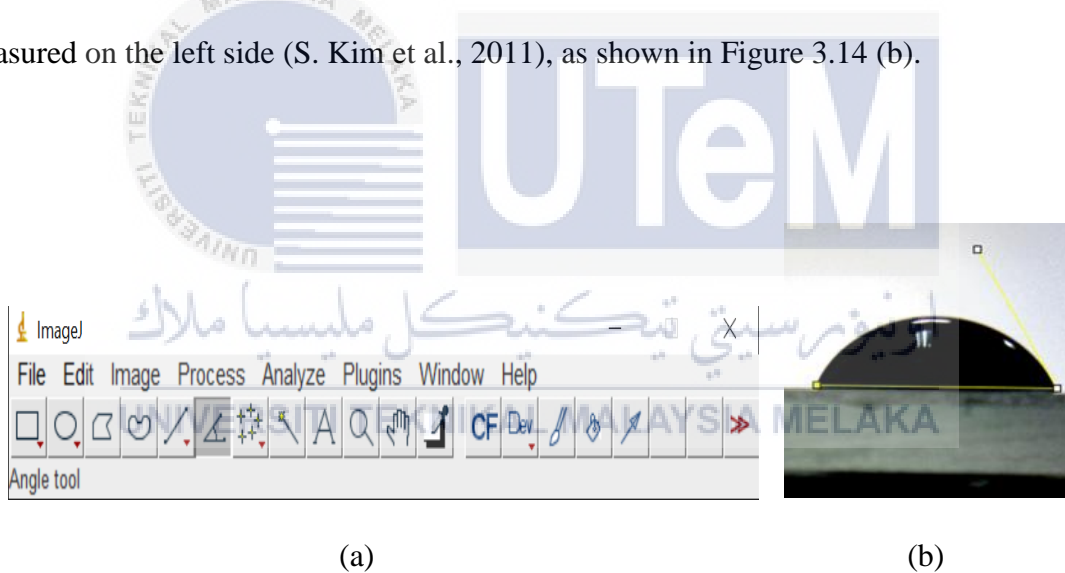


Figure 3.14: (a) ImageJ software (b) Contact angle measured at the right side of ink droplet

3.6 Electrical Characterization

3.6.1 Four probe point test

To explore the influence of filler loading on SCI with a varying substrate, the four-point probe machines were used to measure the sheet resistivity of SCI's samples by following ASTM F390 as a guideline. The machine operates by passing a current (I) through two outer probes, and the Voltage (V) is measured through the inner probes. Thus, the data was obtained is sheet resistivity, R_s in-unit Ω/sq .

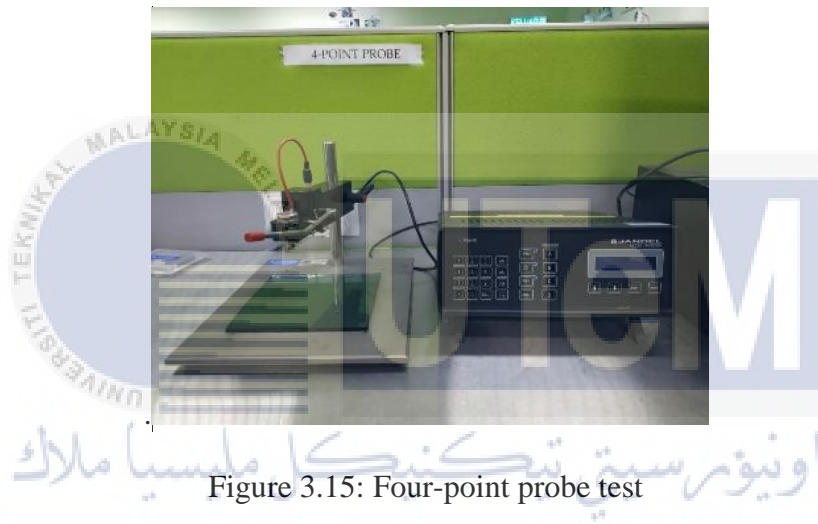


Figure 3.15: Four-point probe test

The current flow through the probe was set at a specified ampere before the resistivity test. Then, each sample was placed aligned and under a four-point probe head, as illustrated in Figure 3.16, and the probe head was lifted down until it touched the sample.

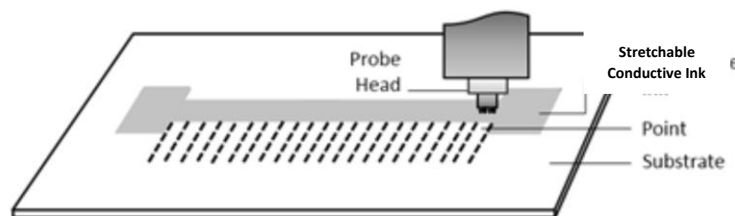


Figure 3.16: Illustration of probe head is placed on top of SCI surface (Ashikin et al., 2018)

The sheet resistance calculation is expressed in Eq. (3.6):

$$R_s = G \times \frac{V}{I} \quad (3.6)$$

Where correlation factor (G) is assumed to be 4.53 (Ashikin et al., 2018).

To evaluate the precision level on R_s analysis, the R_s value was taken two times for each point, and the average of R_s was calculated.

3.7 Mechanical Characterization

3.7.1 180° Peel test

The evaluation of adhesion strength between different filler loading of SCI with TPU and PET substrate was analysed by the 180° Peel test. The Universal Tensile Machine with a 50N load cell was used (SHIMADZU AGS-X-HC Machine), as shown in Figure 3.17. The machines measure the force (N) and the displacement of the upper grip during the test (mm). The peel test results provide the bond strength of the sample (N/mm).



Figure 3.17: 50 N Universal Tensile Machine (SHIMADZU AGS-X-HC)

The glass slide and substrate were attached to the top and bottom grip of tensile test jigs, respectively, as presented in Figure 3.18. The width of the sample was set at 20 mm, and the samples were pulled at a speed of 10 mm/min.

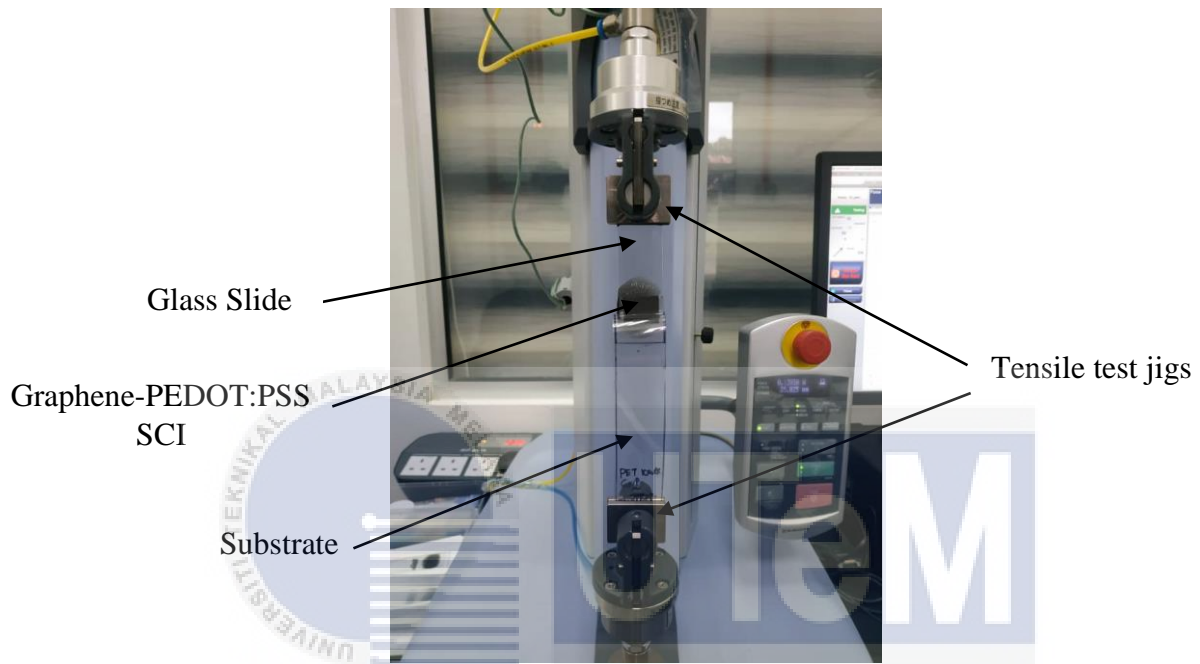


Figure 3.18: Close-up view of sample set-up

The peel test results were recorded, and the average bond strength (N/mm) for each sample was calculated. The bond strength of the sample (N/mm) calculation is expressed in Eq. (3.7):

$$Adhesion\ Strenght = \frac{Measured\ Force\ (N)}{Width\ of\ the\ sample\ (mm)} \quad (3.7)$$

CHAPTER 4

RESULTS AND DISCUSSION

4.1 Introduction

This section discusses the results obtained from the experimental works described in Chapter 3 Methodology. The results are focused on fulfilling this project's objectives, which addressed the effect of different Graphene-PEDOT: PSS SCI filler loading on its functional properties with varying substrates.

4.2 Viscosity of SCI with varying filler loading

This section consists of results and discussion on the velocity of Graphene-PEDOT: PSS ink with varying Graphene filler loading. Thus, the relation between the viscosity of the SCI and the electrical performance with varying substrates can be made.

The viscosity test on SCI with GNP filler loading of 5 wt.%, 7.5 wt.%, and 10 wt.% were measured using a digital viscometer (MODEL 52DV). However, it was not possible to measure the SCI with 10 wt.% GNP, possibly since it is a much higher filler ink concentration. Table 4.1 illustrates the results of the viscosity of SCI with 5 wt. % and 7.5 wt. %.

Table 4.1: Graphene filler loading and viscosity of SCI

Graphene filler loading, wt.%	Viscosity, mPa.s
5	26
7.5	238
10	N/A

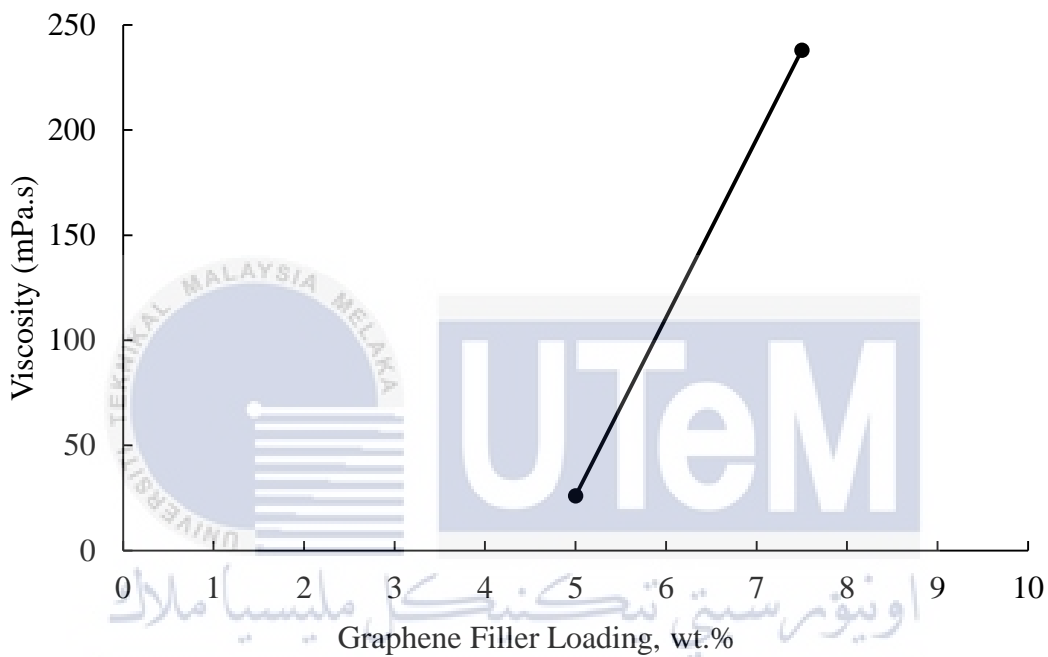


Figure 4.1: Viscosity against filler loading of Graphene-PEDOT: PSS SCI

Based on Figure 4.1, viscosity increase when filler loading increase from 5 wt. % to 7.5 wt.%. As expected, an increase in filler loading directly increases the SCI concentration and contributes to higher viscosity. It is because the fluid concentration is directly proportional to the viscosity. According to Psimadas et al. (2012), increasing the solute concentration will increase viscosity simply due to the need for additional energy to translate or rotate these molecules in solution.

Based on the results shown in Table 4.1, the viscosity of the SCI with 5 wt.% GNP filler loading suggest that it may be suitable for the Piezo inkjet printing technique. The reason is that the viscosity value of 26 mPa.s is categorized as low viscosity ink. Based on the previous research by Öhlund et al. (2014), the viscosity from 5 to 30 mPa.s is appropriate for the Piezo inkjet printing method. In addition, the viscosity results for the SCI with 7.5 wt.% GNP filler loading, which is 238 mPa.s, suggest that the ink exhibit a middle-high viscosity, making it ideal for Flexography printing (Khan et al., 2020).

4.3 Hydrophobicity study of different SCI's filler loading on PET and TPU substrate.

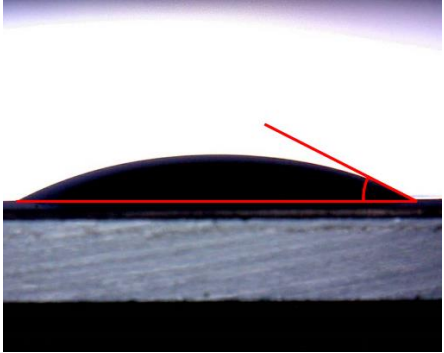
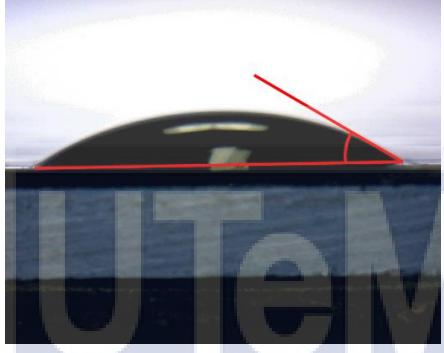

Currently, Printed Flexible Circuits (PFC) substrates such as Polyethylene Terephthalate (PET) and Thermoplastic Polyurethane (TPU) are two examples of polymer substrates that are finding increasing demand in flexible electronic applications. Although theoretically, the PET and TPU are polymer substrates, the main difference is that TPU features flexibility and stretchability characteristics while PET is flexible but not stretchable. Therefore, it is essential to study the hydrophobicity performances of SCI on these polymer substrates. Furthermore, instabilities between the ink and the substrate are a crucial problem that can cause printed layers to exfoliate (Kim et al., 2011).

The contact angle test on the SCI with 5 wt.% and 7.5 wt.% Graphene filler loading on PET and TPU substrate were conducted using a self-fabricated contact angle measuring tool. In contrast, the SCI with 10 wt.% GNP filler loading was not measured for both substrates. As a result, the ink droplet behaviour is not spherical, and there is a high ink concentration. The findings attained from the experiment is shown in Table 4.2 and Table 4.3.

Table 4.2: SCI droplet behaviour on PET and the average contact angle.

Substrates	Graphene Filler Loading wt.%	Droplet Ink Behaviour	Average Contact Angle ($^{\circ}$) (θ)
PET	5		28.052 ± 5.05
	7.5		31.502 ± 0.841
	10		N/A

Table 4.3: Ink droplet behaviour on TPU and the average contact angle.

Substrates	Graphene Filler Loading wt. %	Droplet Ink Behaviour	Average Contact Angle (°) (θ)
TPU	5		28.052 ± 5.05
	7.5		31.502 ± 0.841
	10		N/A

Referring to Table 4.2 and Figure 4.3, the SCI with 5 wt.% GNP filler loading is lower than 7.5 wt.% GNP filler loading deposited onto both the PET and TPU substrates. Such observation could be due to higher filler loading, causing the SCI concentration to increase and directly increase the contact angle. A similar trend is reported in the literature, in which it was argued that the higher the ink concentration, the higher the contact angle (Kim et al., 2011). Nonetheless, Kang et al. (2009) stated that the ink concentration must be controlled to remain within a range suitable for the electric function because the smaller contact angles provide higher ink transfer rates.

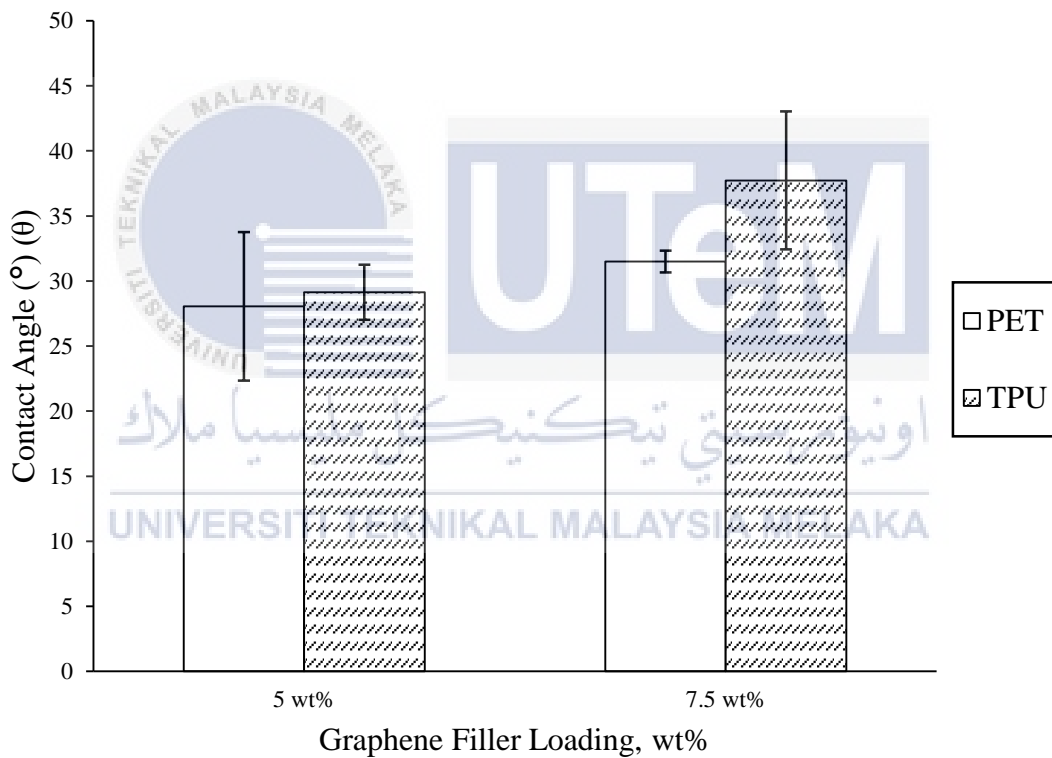


Figure 4.2: Average Contact Angle of SCI printed on different substrate Vs GNP filler loading

Based on Figure 4.2, at a filler loading of 5 wt.%, there is a 4% difference in the contact angle between PET and TPU substrate. Moreover, at increasing GNP filler loading, that is at 7.5 wt.%, there is a much more significant difference of 20%. This finding suggests that the SCI is more hydrophilic on the PET substrate than onto the TPU substrate with increasing filler loading. One of the significant differences is because both substrates are made from different polymer materials based; on which PET is made of ethylene, while TPU is made of urethane. According to Hansen (2007), the urethane base polymer has lower surface energy than ethylene base due to polar/dispersion interaction that can be translated into higher surface tension and contact angle. Hence, TPU has a larger contact angle than PET due to the lower surface energy.

4.4 Electrical Performances of different SCI's filler loading on PET and TPU substrate.

In this section, the electrical performance of the SCI with different GNP filler loading on PET and TPU substrates is explained based on sheet resistance measurement using JANDEL In-line Four Point Probe. Besides, ASTM F390-11 was used as a guideline for this electrical characterization test. First, the sheet resistance of the SCI with different GNP filler loading on PET and TPU substrates was measured. Table 4.4 illustrates the results of the average sheet resistance of the SCI on PET and TPU substrate with 5 wt.%, 7.5 wt.% and 10 wt.% GNP filler loading.

Table 4.4: Graphene filler loading and average sheet resistance of SCI on PET and TPU substrate

Graphene Filler Loading wt.%	Average Sheet Resistivity ($\Omega/\text{sq.}$)	
	PET	TPU
5	9.34 ± 1.22	9.90 ± 1.38
7.5	7.20 ± 0.45	5.81 ± 0.96
10	4.02 ± 0.41	3.97 ± 0.46

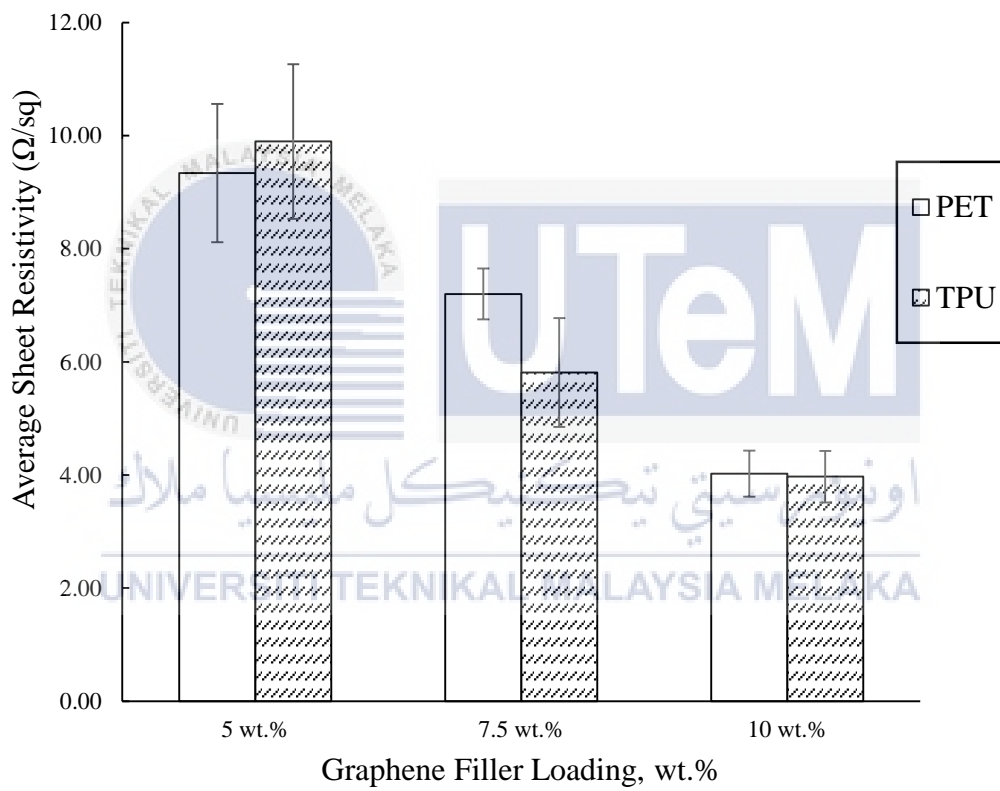


Figure 4.3: Average Sheet Resistance Vs Graphene-PEDOT: PSS SCI with different Graphene filler loading and substrate

Based on Figure 4.3, the sheet resistance for all the samples decreases with increasing GNP filler loading, from 5 wt.% to 10 wt.% for both substrates. As hypothesized earlier, an increase in the GNP filler loading contributes to a lower electrical resistivity in the SCI and directly increase SCI's conductivity since the sheet resistivity is inversely proportional to electrical conductivity. Moreover, between the SCI with GNP filler loading of 5 wt.%, 7.5 wt.%, and 10 wt.% for both substrates, there is a considerable decrease in the sheet resistance, indicating that the percolation threshold has been achieved at this level.

In addition, the sheet resistivity of SCI for 5 wt.% on the TPU substrate is higher than those printed onto the PET substrate, as shown in Figure 4.3. It could be correlated with the viscosity of 5 wt.% GNP filler loading, 26 mPa.s, as reported earlier in Section 4.1. With much lower SCI viscosity, the amount of ink applied to the substrate during stencil printing is uneven. It causes a more extensive contact area between conductive fillers, enhancing resistance. Based on the literature, as the distance between fillers becomes smaller, the resistance decreases and allows a high number of conductive paths fillers to form (Teh et al., 2011). Besides, these results also show that the SCI with very low viscosity is not suitable for using the stencil printing method to print the ink on the substrate because the ink viscosity needed for the stencil printing method is 1000-10000 mPa.s (Öhlund et al., 2014).

However, the sheet resistivity for the SCI with GNP filler loading of 7.5 wt. % and 10 wt.% on TPU substrate are relatively lower than those printed onto the PET substrate. It could be because the TPU substrates are stretchable and have a softer surface than the PET substrate, which is more rigid. According to Ismail et al. (2020), the ink tends to shrink and quickly pulls the TPU substrate to crumple closer during the curing process, causing the contact surface between the particles to increase and decrease the particle gap.

4.5 Adhesion Performances of different SCI's filler loading on PET and TPU substrate.

In this section, the mechanical performance of the SCI with different GNP filler loading on PET and TPU substrates is discussed based on the 180° peel test results under the tensile loading to evaluate the quantitative adhesion analysis between the SCI and a substrate.

Table 4.5: Graphene filler loading and average maximum adhesion strength of SCI on PET and TPU substrate

GNP Filler Loading (wt.%)	Average Maximum Adhesion Strength (N/mm)	
	PET	TPU
5	0.0198 ± 0.0365	0.0156 ± 0.0067
7.5	0.0057 ± 0.0040	0.0042 ± 0.0021
10	0.0056 ± 0.0026	0.0040 ± 0.0019

By referring to Table 4.5, it is shown that the SCI with 5 wt.% GNP filler loading has higher adhesion strength compared to those of 7.5 wt.% and 10 wt.%, for both the PET and TPU substrates. Such observation could be because the SCI filled with 5 wt.% of GNP is properly dispersed with the matrix. However, a further increase in the GNP filler loading from 7.5 wt.% to 10 wt.% has resulted in a slight decrease of adhesion for the SCI printed on both substrates. It might be due to the high viscosity for the SCI with GNP filler loading of 7.5 wt.% and 10 wt.%, which is increased, causing the GNP filler to be aggregated, resulting in poor dispersion and reducing the adhesion strength between the SCI and the substrates (Trinidad et al., 2017). In addition, an increase of conductive filler loading in SCI means volume fraction of matrix relatives to the total volume of SCI reduced. Hence, it caused a decrease in the composite's adhesion strength since the binder is unable to be in continuous form and will not provide a good polymer network (Trinidad et al., 2017).

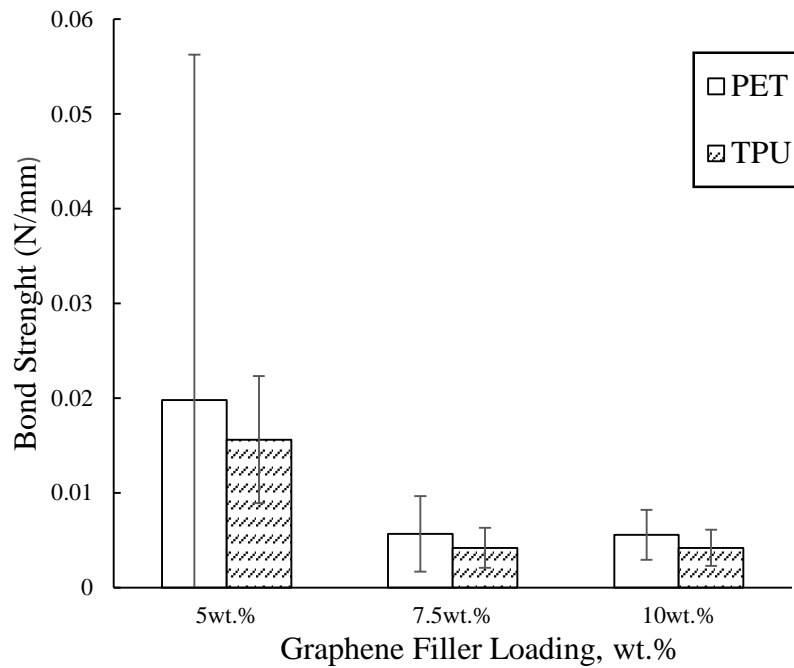


Figure 4.4 Average Maximum Bond Strength Vs Graphene-PEDOT: PSS SCI with different Graphene filler loading and substrate

Based on Figure 4.4, at 5 wt.%, there is a 21.21% difference in the adhesion strength between PET and TPU substrates, while at 7.5 and 10 wt.%, there are 26% and 28.57% differences in the adhesion strength between PET and TPU substrates. It indicates that the SCI exhibit a much higher adhesion strength on PET substrates than TPU substrate. As discussed in Section 4.3, the SCI printed onto the PET substrate is much more hydrophilic than the TPU substrate as the filler loading increases since the contact angle on PET is lower than TPU, which result in high adhesion strength (Geils et al., 2019).

However, the adhesion strength of Graphene-PEDOT: PSS SCI printed on both substrates for all samples is less good compared to commercial conductive ink. Kim et al. (2014) reported that the commercial Ag nano ink has the adhesion strength in the range 0.1-0.2 N/mm. Cruz et al. (2016) suggest that the surface treatment of the polymer substrate is needed to compatibility and improve adhesion forces by increasing the surface tension of the polymer, thus changing their hydrophobicity and increasing the surface contact area.

CHAPTER 5

CONCLUSION AND RECOMMENDATION

5.1 Conclusion

In this study, the effect of different GNP filler loading on the viscosity of Graphene-PEDOT: PSS SCI was carried out through viscosity testing. Moreover, the influence of TPU and PET substrates on the electrical properties with different GNP filler loading was studied through sheet resistance measurements. Finally, the adhesion performances of different SCI's filler loading on PET and TPU substrate was studied through contact angle testing and the 180° peel test.

In terms of the electrical characterization, as the filler loading increases, the sheet resistance of the SCI printed on TPU and PET substrate decreases, indicating good conductivity. The SCI printed on the TPU substrate has better conductivity than the SCI printed on the PET substrate. This is because the TPU substrates are stretchable and have a softer surface than PET substrate, which is more rigid. However, the sheet resistivity of SCI with lower filler loading on the TPU substrate is higher than those printed onto the PET substrate because of lower viscosity. From the results obtained, the SCI with low viscosity is inappropriate with the stencil printing method and may affect the electrical properties of the printed SCI on the substrate.

For the 180° peel test, SCI exhibited higher adhesion strength on PET substrates than TPU substrates. It is due to SCI printed on PET substrates being more hydrophilic than TPU substrates because the filler loading is increased due to the contact angle on PET being lower than TPU, which results in high adhesion strength. However, the adhesion strength of Graphene-PEDOT: PSS SCI printed on PET and TPU substrates is less good compared to other commercial inks. It may be due to the low surface tension of the PET and TPU substrates received, causing the lower surface contact area between the SCI and the substrate.

From the results obtained in this research, it can be concluded that the SCI printed on different substrates affect the functional properties of the SCI. Besides, the SCI's viscosity and the SCI's hydrophobicity on the substrates play a vital role in determining the SCI's good electrical and mechanical properties.

5.2 Recommendation

For further improvement in this study, SCI surface morphology on substrates should be performed through Scanning Electron Microscope (SEM). It plays an essential role in observing the texture, chemical composition, structure, and constituents between SCI and polymer substrate. Moreover, the adhesion strength between SCI and the polymer substrate, especially on the stretchable substrate, can be further improved by performing surface treatment on the substrate. It can increase the adhesion by increasing the surface tension of the polymer, changing its hydrophobicity, and increasing the surface contact area (Cruz et al., 2016). Finally, the SCI printing technique shall be performed according to the viscosity of the SCI since the viscosity of the SCI and printing techniques are closely related to each other.

REFERENCES

- Ashikin, A. S., Omar, G., Tamaldin, N., Kamarolzaman, A. A., Jasmee, S., & Ani, F. C. (2018). *Comparative Study on the Polyethylene Terephthalate (Pet) and Thermoplastic Polyurethane (Tpu) As Substrate Materials for Conductive Ink*. xx(January).
- Azani, M. R., Hassanpour, A., & Torres, T. (2020). Benefits, Problems, and Solutions of Silver Nanowire Transparent Conductive Electrodes in Indium Tin Oxide (ITO)-Free Flexible Solar Cells. In *Advanced Energy Materials* (Vol. 10, Issue 48, p. 2002536). Wiley-VCH Verlag. <https://doi.org/10.1002/aenm.202002536>
- Aziz, N. A., Saad, A. A., Ahmad, Z., Zulfiqar, S., Ani, F. C., & Samsudin, Z. (2020). Stress analysis of stretchable conductive polymer for electronics circuit application. *Handbook of Materials Failure Analysis*, April, 205–224. <https://doi.org/10.1016/b978-0-08-101937-5.00008-7>
- Cataldi, P., Athanassiou, A., & Bayer, I. S. (2018). Graphene nanoplatelets-based advanced materials and recent progress in sustainable applications. *Applied Sciences (Switzerland)*, 8(9). <https://doi.org/10.3390/app8091438>
- Choi, S., Han, S. I., Kim, D., Hyeon, T., & Kim, D. H. (2019). High-performance stretchable conductive nanocomposites: Materials, processes, and device applications. *Chemical Society Reviews*, 48(6), 1566–1595. <https://doi.org/10.1039/c8cs00706c>
- Cruz, S., Rocha, L. A., & Viana, J. C. (2016). Enhanced printability of thermoplastic polyurethane substrates by silica particles surface interactions. *Applied Surface Science*, 360, 198–206. <https://doi.org/10.1016/j.apsusc.2015.10.094>

- Ding, Y., Wang, X., Guo, Z., Mo, L., Wang, W., & Li, L. (2020). Application of Stretchable Conductive Ink in the Field of Flexible Electronic Devices. In P. Zhao, Z. Ye, M. Xu, & L. Yang (Eds.), *Advanced Graphic Communication, Printing and Packaging Technology* (pp. 702–714). Springer Singapore.
- Doshi, B., Sillanpää, M., & Kalliola, S. (2018). A review of bio-based materials for oil spill treatment. *Water Research*, *135*, 262–277.
<https://doi.org/10.1016/j.watres.2018.02.034>
- Eitner, U., & Rendler, L. C. (2016). The Impact of Ribbon Properties on Measured Peel Forces. *Energy Procedia*, *92*, 500–504. <https://doi.org/10.1016/j.egypro.2016.07.133>
- Geils, J., Patzelt, G., & Kesel, A. (2019). The larger the contact angle , the lower the adhesion? *Bionik Pat. Aus Der Natur. Innov. Für Technol.*, 188–195.
- Gould, P. (2003). Smart, clean surfaces. *Materials Today*, *6*(11), 44–48.
[https://doi.org/10.1016/S1369-7021\(03\)01131-3](https://doi.org/10.1016/S1369-7021(03)01131-3)
- Hashemi, S. A., & Mousavi, S. M. (2016). Effect of bubble based degradation on the physical properties of Single Wall Carbon Nanotube/Epoxy Resin composite and new approach in bubbles reduction. *Composites Part A: Applied Science and Manufacturing*, *90*, 457–469. <https://doi.org/10.1016/j.compositesa.2016.08.015>
- Hong, S., Lee, H., Lee, J., Kwon, J., Han, S., Suh, Y. D., Cho, H., Shin, J., Yeo, J., & Ko, S. H. (2015). Highly Stretchable and Transparent Metal Nanowire Heater for Wearable Electronics Applications. *Advanced Materials*, *27*(32), 4744–4751.
<https://doi.org/10.1002/adma.201500917>
- Hsu, C. P., Guo, R. H., Hua, C. C., Shih, C. L., Chen, W. T., & Chang, T. I. (2013). Effect of polymer binders in screen printing technique of silver pastes. *Journal of Polymer*

Research, 20(10). <https://doi.org/10.1007/s10965-013-0277-3>

Hu, L., Song, J., Yin, X., Su, Z., & Li, Z. (2020). Research Progress on Polymer Solar Cells Based on. *Polymer*, 12(145), 1–19.

Huang, Q., & Zhu, Y. (2019). Printing Conductive Nanomaterials for Flexible and Stretchable Electronics: A Review of Materials, Processes, and Applications. *Advanced Materials Technologies*, 4(5), 1–41.

<https://doi.org/10.1002/admt.201800546>

Hunrath, C., & Forest, L. (2009). *Circuit Technology Crossovers Where PCBs and Printed Electronics Meet. IPC APEX EXPO Conference Proceedings*, 6.

Ismail, N., Salim, M. A., Naroh, A., Masripan, N. A., Saad, A. M., Sudin, M. N., & Caridi, F. (2020). Resistivity characterization for carbon based conductive nanocomposite on polyethylene terephthalate and thermoplastic polyurethane substrates. *International Journal of Nanoelectronics and Materials*, 13(Special Issue ISSTE 2019), 315–326.

Jason, N. N., Shen, W., & Cheng, W. (2015). Copper Nanowires as Conductive Ink for Low-Cost Draw-On Electronics. *ACS Applied Materials and Interfaces*, 7(30), 16760–16766. <https://doi.org/10.1021/acsami.5b04522>

Kausar, A. (2017). Role of Thermosetting Polymer in Structural Composite. *American Journal of Polymer Science & Engineering*, 5(1), 1–12.
http://www.ivyunion.org/index.php/ajpse/article/view/1050/pdf_34

Khan, Y., Thielens, A., Muin, S., Ting, J., Baumbauer, C., & Arias, A. C. (2020). A New Frontier of Printed Electronics: Flexible Hybrid Electronics. *Advanced Materials*, 32(15), 1–29. <https://doi.org/10.1002/adma.201905279>

Kim, D. C., Shim, H. J., Lee, W., Koo, J. H., & Kim, D. H. (2020). Material-Based

- Approaches for the Fabrication of Stretchable Electronics. *Advanced Materials*, 32(15), 1–29. <https://doi.org/10.1002/adma.201902743>
- Kim, S., Kang, H. W., Lee, K. H., & Sung, H. J. (2011). Effect of hydrophobic microstructured surfaces on conductive ink printing. *Journal of Micromechanics and Microengineering*, 21(9). <https://doi.org/10.1088/0960-1317/21/9/095026>
- Lauren, S. (2019). What is wettability? *Biolin Scientific*, 1–9. <https://www.biolinscientific.com/blog/what-is-wettability>
- Lim, C. K., Lee, Y. S., Choa, S. H., Lee, D. Y., Park, L. S., & Nam, S. Y. (2017). Effect of Polymer Binder on the Transparent Conducting Electrodes on Stretchable Film Fabricated by Screen Printing of Silver Paste. *International Journal of Polymer Science*, 2017. <https://doi.org/10.1155/2017/9623620>
- Merilampi, S., Björninen, T., Haukka, V., Ruuskanen, P., Ukkonen, L., & Sydänheimo, L. (2010). Analysis of electrically conductive silver ink on stretchable substrates under tensile load. *Microelectronics Reliability*, 50(12), 2001–2011. <https://doi.org/10.1016/j.microrel.2010.06.011>
- Mohammed, A., & Pecht, M. (2016). A stretchable and screen-printable conductive ink for stretchable electronics. *Applied Physics Letters*, 109(18). <https://doi.org/10.1063/1.4965706>
- Öhlund, T., Gane, P. P., Olin, H. P., Nilsson, H.-E. P., Andersson, M. D., Örtengren, J., Andersson, H., Nilsson, H.-E., Andersson, M., Forsberg, S., Schuppert, A., Andres, B., Schmidt, W., Zhang, R., Olin, H., Hummelgård, M., & Bäckström, J. (2014). *Metal Films for Printed Electronics : Ink-substrate Interactions and Sintering* (Issue December 2014).

- Onggar, T., Kruppke, I., & Cherif, C. (2020). Techniques and processes for the realization of electrically conducting textile materials from intrinsically conducting polymers and their application potential. *Polymers*, *12*(12), 1–46.
<https://doi.org/10.3390/polym12122867>
- Psimadas, D., Georgoulas, P., Valotassiou, V., & Loudos, G. (2012). Molecular Nanomedicine Towards Cancer : *Journal of Pharmaceutical Sciences*, *101*(7), 2271–2280. <https://doi.org/10.1002/jps>
- Qi, D., Zhang, K., Tian, G., Jiang, B., & Huang, Y. (2021). Stretchable Electronics Based on PDMS Substrates. *Advanced Materials*, *33*(6), 1–25.
<https://doi.org/10.1002/adma.202003155>
- Saad, H., Salim, M. A., Azmmi Masripan, N., Saad, A. M., & Dai, F. (2020). Nanoscale graphene nanoparticles conductive ink mechanical performance based on nanoindentation analysis. *International Journal of Nanoelectronics and Materials*, *13*(Special Issue ISSTE 2019), 439–448.
- Seekaew, Y., Lokavee, S., Phokharatkul, D., Wisitsoraat, A., Kerdcharoen, T., & Wongchoosuk, C. (2014). Low-cost and flexible printed graphene-PEDOT:PSS gas sensor for ammonia detection. *Organic Electronics*, *15*(11), 2971–2981.
<https://doi.org/10.1016/j.orgel.2014.08.044>
- Trinidad, J., Chen, L., Lian, A., & Zhao, B. (2017). Solvent presence and its impact on the lap-shear strength of SDS-decorated graphene hybrid electrically conductive adhesives. *International Journal of Adhesion and Adhesives*, *78*, 102–110.
<https://doi.org/10.1016/j.ijadhadh.2017.06.012>
- Wagner, S., & Bauer, S. (2012). Materials for stretchable electronics. *MRS Bulletin*, *37*(3), 207–213. <https://doi.org/10.1557/mrs.2012.37>

Wang, C. L., Hsieh, J., Lee, L. W., Wu, J. Y., Hsiao, P. Y., Chu, J. H., & Wang, C. M. (2019). An Unprecedented Interpenetrating Structure Built from Two Differently Bonded Frameworks: Synthesis, Characteristics, and Efficient Removal of Anionic Dyes from Aqueous Solutions. *Chemistry - A European Journal*, 25(33), 7815–7819. <https://doi.org/10.1002/chem.201900607>

White, H. J. (1989). Amine curing agents for epoxy resins. *Journal of Protective Coatings and Linings*, 6(8), 47–56.

Yunos, A. M., Omar, G., Salim, M. A., Masripan, N. A., Cosut, B., & Adnan, A. F. M. (2020). Temperature dependence on silver conductivity and adhesion performance between silver and flexible substrate. *Journal of Advanced Research in Fluid Mechanics and Thermal Sciences*, 73(2), 73–87. <https://doi.org/10.37934/ARFMTS.73.2.7387>

Yurenka, S. (1962). Peel testing of adhesive bonded metal. *Journal of Applied Polymer Science*, 6(20), 136–144. <https://doi.org/10.1002/app.1962.070062004>

UNIVERSITI TEKNIKAL MALAYSIA MELAKA